Journal of the Iranian Chemical Society (2019) 16:2587–2612
https://doi.org/10.1007/s13738-019-01723-1

ORIGINAL PAPER

Carbon-based nanocatalyst: An efficient and recyclable heterogeneous catalyst for one-pot synthesis of *gem*-bisamides, hexahydroacridine-1,8-diones and 1,8-dioxo-octahydroxanthenes

Jaspreet Kour[1] · Monika Gupta[1] · Bushra Chowhan[1] · Vivek K. Gupta[2]

Received: 4 September 2018 / Accepted: 23 June 2019 / Published online: 18 July 2019

Abstract

In this abstract, we discuss the progress related to sulfonated carbon-based materials in various acid-catalyzed organic transformations which are then further utilized in medicinal field, laboratories and industries. A simple and novel methodology was employed to prepare carbon-based nanocatalyst, i.e. cellulose[2-(sulfooxy)ethyl]mercaptosulfonic acid as a solid acid catalyst. This nanocatalyst is recyclable and also exhibited very high activity. Novel carbon-based nanocatalyst, i.e. cellulose[2-(sulfooxy)ethyl]mercaptosulfonic acid[SEMSA] was successfully synthesized by reacting mercaptoethanol and chlorosulfonic acid, and the catalytic activity of the prepared catalysts was evaluated for the one-pot synthesis of *gem*-bisamides from various aldehydes and benzamide, hexahydroacridine-1,8-diones via three-component condensation of aromatic aldehyde, dimedone and ammonium acetate or aromatic amine and 1,8-dioxo-octahydroxanthenes using aldehyde and dimedone. Application of this new heterogeneous nanocatalyst system offered the advantages of high yields, short reaction times, eco-friendly nature and easy work-up procedure compared to the conventional methods of the synthesis, and confirmation of products synthesized has been done using studies like ^{1}H NMR and ^{13}C NMR. Among the various catalysts, this nanocatalyst, i.e. cellulose [2-(sulfooxy)ethyl]mercaptosulfonic acid[SEMSA], was found to be the most active and selective and could be recycled several times without significant loss of activity. Also, scanning electron microscopy and transmission electron microscopy of the catalyst have been performed to know the internal and external morphology, size, thermogravimetric analysis to study the thermal stability and Fourier transform infrared spectroscopy to study the modification pattern of the catalyst have been undertaken and presented in this work. Due to its simple and inexpensive solid support, i.e. cellulose and environmentally benign toluene, ethanol and acetonitrile as solvents in three different transformations which are less toxic, easily available and less expensive than other solvents.

Electronic supplementary material The online version of this article (https://doi.org/10.1007/s13738-019-01723-1) contains supplementary material, which is available to authorized users.

✉ Monika Gupta
monika.gupta77@rediffmail.com

Jaspreet Kour
kourhpjaspreet.88@gmail.com

Bushra Chowhan
bushrachowhan341@gmail.com

Vivek K. Gupta
vivek.gupta2k9@gmail.com

[1] Department of Chemistry, University of Jammu, Jammu 180 006, India

[2] Department of Physics, University of Jammu, Jammu 180 006, India

Graphic abstract

We reported here a novel route for the synthesis of *gem*-bisamides, hexahydroacridine-1,8-diones and 1,8-dioxo-octahydroxanthenes

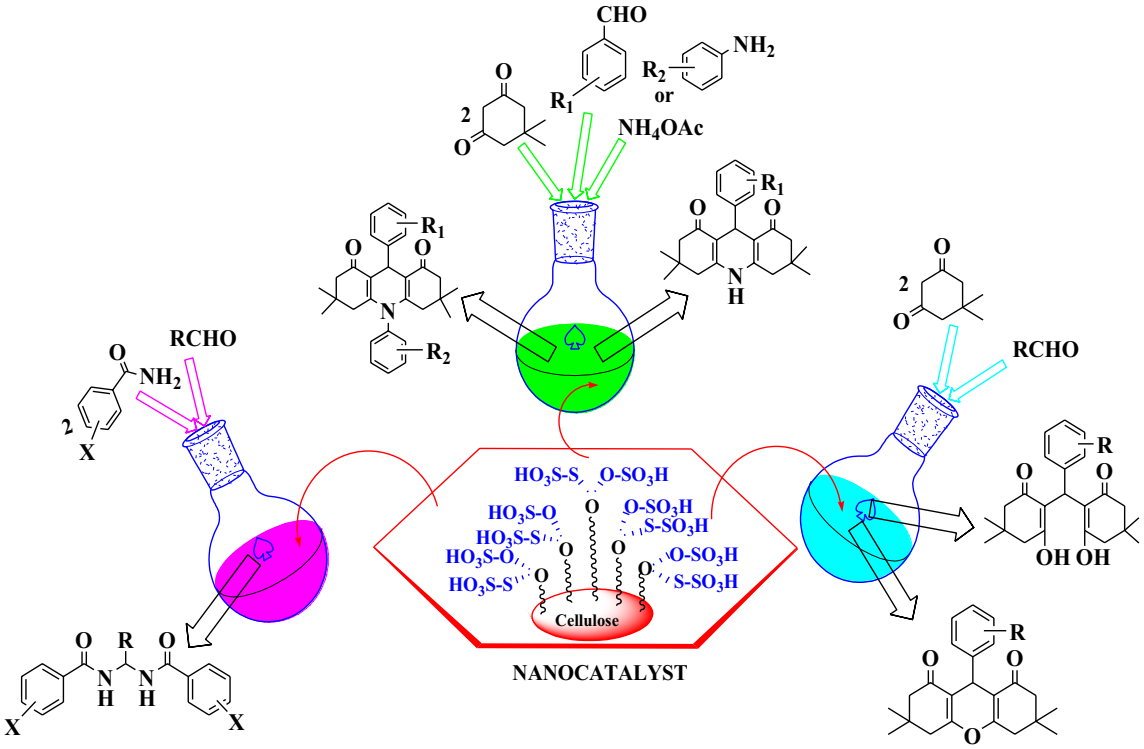

Keywords Solid acid · Catalyst · Mercaptoethanol · Acridines · Dimedone · Xanthenes · SEMSA

Introduction

Recent interest in design and development of nanocatalysis has gained a greater scope for designing of nanocatalysts with more efficiency, high stability and greater selectivity. Nanocatalysts are highly selective and reactive than their bulk counterparts or the conventional catalysts. Nanotechnology has been of great use now-a-days because of their extremely small size and larger surface area-to-volume ratio providing more active catalytic sites which helps in designinig of novel heterogeneous solid acid catalysts [1]. Catalysis has played a very important role in the development of green industry of new century [2]. Lewis and Bronsted acid catalysts represent an important class that are used in the large-scale production of fine chemicals as well as industrial chemicals [3]. Bronsted acids have been widely utilized as efficient catalysts for numerous organic transformations. The most straight forward and a common approach used to promote a chemical reaction is by means of a Bronsted acid [4]. Now-a-days, heterogeneous solid acid catalysts are of paramount importance for the synthesis of organic compounds due to their handling, no toxicity and recyclability [5] in comparison with homogeneous catalysts because of their difficulty in separation, high volatility, toxicity, waste generation and limited solubility/phase contact with the starting materials. Chemical industries are forced to consider environmental aspects, therefore, it becomes necessary to replace liquid acid with solid acid [6–8]. In recent years, uses of catalyst supported on solid supports have been extensively developed because such catalysts not only cause to simply the purification processes but also do not release toxic substances residues into the environment. Although some of them are sensitive to moisture and can be easily decomposed, application of them in organic reactions is difficult. This problem can be solved by fixed onto solid supports [9–11] such as silica, starch, cellulose, zeolites, montmorillonite, aluminas attracts the candidates to explore for supported catalysis. Solid support is a material with high surface area to which a catalyst is affixed. The reaction of heterogeneous catalysts occurs at the surface of atoms. Various solid supports especially cellulose was being used to prepare nanocatalysts or bionanocomposites which were then used to synthesize many organic compounds such as benzodiazepine derivatives,

nitration of aromatic compounds, tetrazolo[1,5-*a*]pyrimidines, chromene-linked nicotinonitriles, pyranopyrimidines and pyrazolopyranopyrimidines, carboxycoumarins, selective conversions of alcohols and alkenes to aldehydes, ketones and epoxides, dihydropyridines and polyhydroquinolines which were of great utility in many fields [12–20]. Consequently, great efforts are being made to maximize the surface area of a catalyst by distributing it over the support. Carbon-based catalysts have great applications in organic syntheses and in industrial manufacturing of materials due to its very useful properties such as resistance to acidic and basic conditions, tunability of surface chemistry, low cost, good electric conductivity and stability against various chemical environments [21–28]. Recently, it was found that solid acid catyalysts have great activity, selectivity and stability [29, 30]. Various catalysts such as ionic liquids, acids, bases, homogeneous catalysts and magnetic nanoparticles have been used for the preparation of different organic compounds but each of these catalysts suffers from some disadvantages such as high cost, harsher conditions, high toxicity, hazardous for environment and longer reaction times. So, our present work on carbon-based nanosolid acid catalysts removes many of these limitations and have been used for the synthesis of *gem*-bisamides from various aldehydes and benzamide, hexahydroacridine-1,8-diones via three-component condensation of aromatic aldehyde, dimedone and ammonium acetate or aromatic amine and 1,8-dioxo-octahydroxanthenes using aldehyde and dimedone.

Amide and bisamide functionalized moieties represent important biological and medicinal scaffolds. Further, symmetrical and unsymmetrical *N,N*-alkylidene bisamides and their derivatives are found as key structural subunits for the construction of peptidomimetic frameworks [31]. Exceptional properties of amide bond offer many vital roles to amide derivatives as biochemicals, structural subunit of polymers and stable synthetic intermediates in chemistry and materials science [32–34]. The most important and interesting moiety, i.e. amide skeleton which is present in the protein molecules, plays a major role in the development and composition of biological and pharmacological systems [35, 36]. They can be easily transformed into other useful materials (such as *gem*-diaminoalkyl and aminoalkyl groups) and are of considerable interest in the synthesis of pharmacological materials such as peptidomimetic compounds [37–42]. Various methods have been reported for the synthesis of bisamides using different catalysts [43–51]. Herein, we report a convenient and efficient method to prepare *gem*-bisamides by condensing different aldehydes with benzamide, using carbon-based nanocatalyst, i.e. cellulose-supported [2-(sulfooxy)ethyl] mercaptosulfonic acid[SEMSA] as an efficient catalyst.

Acridine derivatives have shown many biological activities such as anti-bacterial, cytotoxic, anti-fungal and anti-malarial activities [52–55]. Polycyclic acridine skeletons fused with a five- or six-membered rings have been synthesized extensively studied because they play important role in some DNA intercalating anticancer drugs [56, 57]. The acridine motif is also found in chemosensors, dyes, fluorescent probes and as ligands in metal-promoted catalysis or very recently in hole transport or chiroptical materials and in the two-photon absorption devices [58]. Many earlier methods have been reported to synthesize hexahydroacridine-1,8-diones [59–71], but the most successful one employed is by using nano-carbon-based catalyst, i.e. cellulose-supported [2-(sulfooxy)ethyl]mercaptosulfonic acid[SEMSA].

Xanthene derivatives have attracted considerable attention in recent years because of the pharmaceutical and biological properties. Among the heterocyclic family, xanthene core and its derivatives serve as an important class of compounds, as it is present in natural products with broad biological activities [72, 73]. Several functionalized 1,8-dioxo-octahydroxanthene derivatives possess the significant synthetic interest as they exhibit anti-cancer, anti-plasmodial, anti-viral, anti-bacterial and anti-inflammatory activities [74]. Besides, these heterocyclic molecules have been widely used as luminescent dyes [75], sensitizers in photodynamic therapy [76], in laser technology [77] as well as pH-sensitive fluorescent materials [78]. There are several methods reported for the synthesis of xanthenes derivatives using different catalysts such as sulfuric acid or hydrochloric acid, $InCl_3$/ionic liquid, $SmCl_3$, Fe^{+3} montmorillonite, amberlyst-15, $FeCl_3$/[bmim][BF_4], *p*-dodecylbenzenesulfonic acid, sulfamic acid, $HClO_4/SiO_2$ and trimethylsilyl chloride (TMSCl) [79–93]. However, most of the reported methods suffer many problems such as expensive reagents, hazardous organic solvents, longer reaction time and tedious work-up. In this paper, we reported a novel and facile methodology for the synthesis of *gem*-bisamides from benzamide and aldehyde using nano-carbon based catalyst, hexahydroacridine-1,8-diones from dimedone, aldehyde, ammonium acetate or aromatic amine using recyclable nano catalyst and 1,8-dioxo-ocatahydo xanthenes by the condensation of aromatic aldehyde and dimedone using nano-carbon-based catalyst, i.e. cellulose [2-(sulfooxy)ethyl]mercaptosulfonic acid [SEMSA] as recyclable catalyst.

Experimental

General remarks

All starting materials were purchased from commercial sources and used without further purification. The ^{1}H and ^{13}C NMR data were recorded in $CDCl_3$ or DMSO-d_6 or $CDCl_3$ + DMSO-d_6 on Bruker Avance III (400 MHz) spectrometer. The FTIR

spectra were recorded on Perkin-Elmer. SEM images were recorded using SEM JSM-7600F scanning electron microscope, and transmission electron micrographs (TEM) were recorded on Philips CM-200. TGA-DTA was conducted on a Linseis STA PT-1000 (Germany) thermal analyzer.

Preparation of nanocatalyst cellulose[2-(sulfooxy) ethyl]mercaptosulfonic acid

Pre-treatment of cellulose was carried out by keeping it in an oven for overnight. This activated cellulose was kept aside for sometime. Firstly, 2-mercaptoethanol (1.527 g, 25 mmol) was taken in a flask and chlorosulfonic acid (5.83 g, 3.4 mL, 50 mmol) was added dropwise at room-temperature. During this addition, HCl evolved immediately. The mixture was stirred for 80 min. after completion of reaction while the residual HCl was eliminated by suction. Then, diethyl ether (or CH_2Cl_2) was used for the washing of the prepared catalyst and helped to remove the unreacted chlorosulfonic acid as shown in Scheme 1. After this, activated cellulose (10 g) which we had prepared by keeping it in oven overnight was mixed with this prepared solution. Finally, a blackish solid material (solid acid) was obtained as shown in images in Fig. 1a, b.

General procedure for the synthesis of *gem*-bisamides

Benzamide (2 mmol) and aldehyde (1 mmol) were dissolved in toluene (2 mL) and to this was added carbon-based nanocatalyst (0.1 g), i.e. cellulose [2-(sulfooxy)ethyl]mercaptosulfonic acid[SEMSA]. This was heated to reflux under a condensed atmosphere and stirred with a magnetic stirrer for the desired time. The reaction was worked-up after the completion as indicated by TLC eluted in pet. ether:ethyl acetate. The work-up involved diluting the reaction mixture with ethyl acetate (20 mL), warming and then filtering off the filtrate to separate the catalyst. This was followed by three times cold water washings and then drying over sodium sulfate overnight. Finally, the sodium sulfate was filtered off and the filtrate was evaporated to obtain the crude product, which gave the pure compound on recrystallization in ethanol. The compounds thus obtained were authenticated by spectral studies like ^{1}H NMR and ^{13}C NMR.

Spectral data of the synthesized compounds

N,N'-Benzylidenebisbenzamide **(3a)** White solid; m.p./lit. m.p. 236–237/237–238 °C [5]; ^{1}H NMR (400 MHz, DMSO-d_6): δ 7.24–7.26 (t, J = 8 Hz, 1H, CH), 7.33–7.34 (t, J = 8 Hz, 1H, ArH), 7.35–7.38 (t, J = 8 Hz, 2H, ArH), 7.46–7.50 (m, 6H, ArH), 7.78–7.80 (d, J = 8 Hz, 2H, ArH), 9.03–9.04 (d, J = 8 Hz, 2H, NH); ^{13}C NMR (100 MHz, DMSO): δ 55.0, 124.7, 122.2, 114.8, 125.5, 133.1, 138.3, 160.4.

N,N'-(4-Methoxybenzylidene)bisbenzamide **(3b)** White solid; m.p./lit. m.p. 230–232/232–234 °C [5]; ^{1}H NMR (400 MHz, DMSO-d_6):δ 3.71 (s, 3H, OCH_3), 6.85–7.02 (t, J = 8 Hz, 1H,

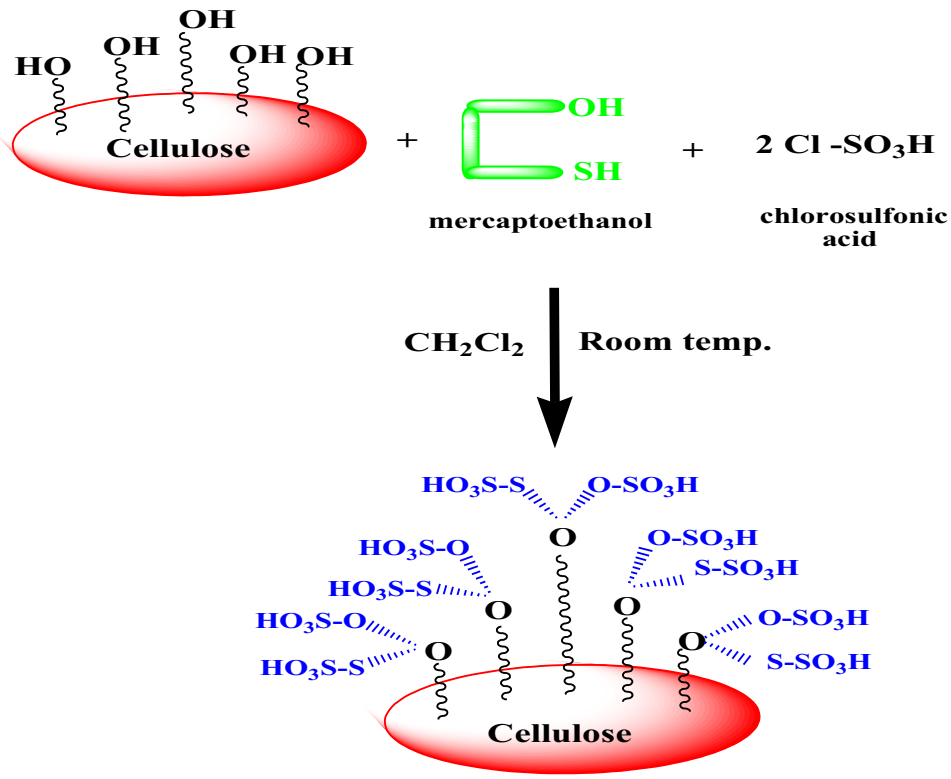

Scheme 1 General scheme for the preparation of cellulose[2-(sulfooxy)ethyl]mercaptosulfonic acid[SEMSA]

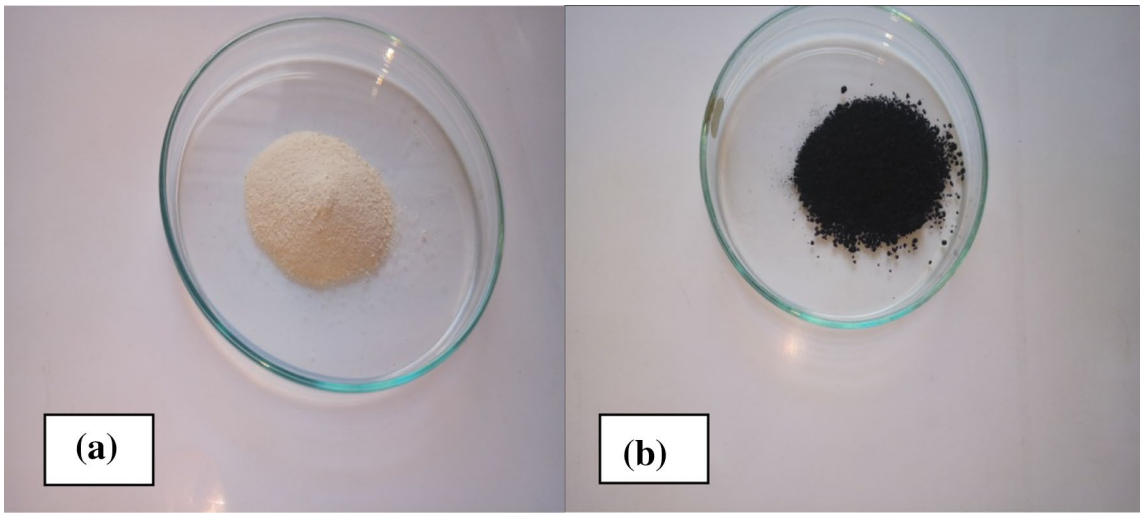

Fig. 1 Images of **a** activated cellulose (creamish in color). **b** Cellulose[2-(sulfooxy)ethyl]mercaptosulfonic acid[SEMSA](black in color)

CH), 7.33–7.54 (m, 10H, ArH), 7.88–7.89 (d, J = 8 Hz, 4H, ArH), 8.42–8.56 (d, J = 8 Hz, 2H, NH); ^{13}C NMR (100 MHz, DMSO-d_6): δ 53.3, 50.9, 103.7, 125.4, 122.4, 131.4, 137.0, 136.1, 156.1, 166.0.

N,N'-(4-Methylbenzylidene)bisbenzamide **(3c)** White solid; m.p./lit. m.p. 245–246/242–243 °C [5]; ^{1}H NMR (400 MHz, DMSO-d_6): δ 2.32(s, 3H, CH_3), 7.04–7.08 (t, J = 8 Hz, 1H, CH), 7.16–7.20 (d, J = 8 Hz, 2H, ArH), 7.35–7.36 (d, J = 8 Hz, 2H, ArH), 7.48–7.59 (m, 6H, ArH), 7.90–7.92 (d, J = 8 Hz, 4H, ArH), 8.90 (d, J = 8 Hz, 2H, NH); ^{13}C NMR (100 MHz, DMSO-d_6): δ 21.2, 53.7, 125.6, 123.2, 120.7, 117.3, 129.0, 133.3, 137.3, 130.8, 162.9.

N,N'-(4-Nitrobenzylidene)bisbenzamide **(3d)** White solid; m.p./lit. m.p. 267–269/265–267 °C [5]; ^{1}H NMR (400 MHz, DMSO-d_6): δ 7.05–7.07 (t, J = 8 Hz, 1H, CH), 7.40–7.55 (m, 6H, ArH), 7.74–7.78 (d, J = 8 Hz, 2H, ArH), 7.90–7.95 (d, J = 8 Hz, 4H, ArH), 8.05–8.09 (d, J = 8 Hz, 2H, ArH), 9.19–9.25(d, J = 8 Hz, 2H, NH); ^{13}C NMR (100 MHz, DMSO-d_6): δ 55.6, 120.9, 123.0, 128.0, 128.5, 127.8, 130.4, 147.7, 147.9, 165.3.

N,N'-(4-Chlorobenzylidene)bisbenzamide **(3e)** White solid; m.p./lit. m.p. 228–229/230–232 °C [5]; ^{1}H NMR (400 MHz, DMSO-d_6): δ 6.95–7.03 (t, J = 8 Hz, 1H, CH), 7.45–7.58 (m, 10H, ArH), 7.92–7.94 (d, J = 8 Hz, 4H, ArH), 9.08–9.10 (d, 2H, J = 8 Hz, NH); ^{13}C NMR (100 MHz, DMSO-d_6): δ 58.0, 125.8, 128.0, 128.3, 128.6, 128.7, 128.0, 130.0, 132.5, 133.1, 136.5, 160.2.

N,N'-(4-Bromobenzylidene)bisbenzamide **(3f)** White solid; m.p./lit. m.p. 255–257/259–260 °C [5]; ^{1}H NMR (400 MHz, DMSO-d_6): δ 6.72–6.76 (t, J = 8 Hz, 1H, CH), 7.40–7.59 (m, 10H, ArH), 7.88–7.90 (d, J = 8 Hz, 4H, ArH), 8.15–8.17 (d, J = 8 Hz, 2H); ^{13}C NMR (100 MHz, DMSO-d_6): δ 57.3, 120.2, 125.2, 125.9, 128.4, 130.8, 134.1, 135.2, 10.9, 140.1.

N,N'-(2-Chlorobenzylidene)bisbenzamide **(3g)** White solid; m.p./lit. m.p. 245–246/242–244 °C [5]; ^{1}H NMR (400 MHz, DMSO-d_6): δ 7.16–7.20 (t, J = 8 Hz, 1H, CH), 7.36–7.40 (t, J = 4 Hz, 2H, ArH), 7.48–7.50 (t, J = 8 Hz, 5H, ArH), 7.54–7.58 (t, J = 4 Hz, 2H, ArH), 7.66–7.69 (d, J = 8 Hz, 1H, ArH), 7.90–7.95 (d, J = 8 Hz, 4H, ArH), 9.10–9.13 (d, J = 8 Hz, 2H); ^{13}C NMR (100 MHz, DMSO-d_6): δ 57.5, 125.5, 127.0, 128.7, 127.9, 128.9, 129.0, 132.0, 130.9, 135.2, 160.5.

N,N'-(3,4-Dimethoxyphenylmethylene)dibenzamide **(3h)** White solid; m.p./lit. m.p. 210–212/216–218 °C [1]; ^{1}H NMR (400 MHz, DMSO-d_6):3.70 (6H, s, OCH_3), 6.90–6.93 (q, 3H, J = 8 Hz), 7.11 (s, 1H), 7.45–7.46 (d, 4H, J = 8 Hz), 7.54–7.56 (d, 2H, J = 4 Hz), 7.84–7.86 (d, 4H, J = 8 Hz), 8.90–8.92 (d, 2H, J = 8 Hz, NH);^{13}C NMR (100 MHz, DMSO-d_6): 164.8, 145.0, 148.0, 131.5, 130.4, 133.2, 131.9, 122.2, 105.9, 112.0.

N,N'-(Furan-2-ylmethylene)bisbenzamide **(3i)** Yellowish solid; m.p./lit. m.p. 202–204/206–208 °C [5]; ^{1}H NMR (400 MHz, DMSO-d_6): δ 7.01–7.05 (t, J = 8 Hz, 1H, CH), 7.26–7.50 (m, 9H, ArH), 7.83–7.85 (d, J = 8 Hz, 4H, ArH), 8.95–8.98 (d, J = 8 Hz, 2H, NH); ^{13}C NMR (100 MHz, DMSO-d_6): δ 59.1, 119.8, 126.7, 127.8, 128.9, 130.3, 134.2, 140.8, 144.5, 152.9, 165.8.

N,N'-(Thiophen-2-ylmethylene)bisbenzamide **(3j)** Yellowish solid; m.p./lit. m.p. 214–215/208–210 °C [5]; ^{1}H NMR (400 MHz, DMSO-d_6): δ 7.00–7.05 (t, J = 8 Hz, 1H, CH),

7.14–7.16 (d, J = 8 Hz, 1H, ArH), 7.20–7.25 (t, J = 8 Hz, 1H, ArH), 7.45–7.55 (m, 7H, ArH), 7.89–7.90 (d, J = 8 Hz, 4H, ArH), 9.15–9.17 (d, J = 8 Hz, 2H, NH); ^{13}C NMR (100 MHz, DMSO-d_6): δ 55.7, 124.0, 123.6, 127.0, 127.5, 124.9, 130.2, 134.0, 160.0.

N,N'-(3-Nitrobenzylidene)bisbenzamide **(3k)** White solid; m.p./lit. m.p. 195–196/190–192 °C [5]; ^{1}H NMR (400 MHz, DMSO-d_6): δ 7.05–7.09 (t, J = 8 Hz, 1H, CH), 7.45–7.50 (m, 6H, ArH), 7.67–7.70 (t, J = 8 Hz, 1H, ArH), 7.93–7.96 (m, 5H, ArH), 8.21–8.23 (d, J = 8 Hz, 1H, ArH), 8.34 (s, 1H, ArH), 9.26–9.28 (d, J = 8 Hz, 2H, NH); ^{13}C NMR (100 MHz, DMSO-d_6): δ 59.3, 121.8, 123.2, 128.0, 128.8, 130.4, 132.2, 134.0, 142.8, 148.2, 166.3.

General procedure for the synthesis of hexahydroacridine-1,8-diones

A mixture of dimedone (2 mmol), aromatic aldehyde (1 mmol), ammonium acetate or aromatic amine (1 mmol) and cellulose[2-(sulfooxy)ethyl]mercaptosulfonic acid[SEMSA] (0.1 g) in the presence of ethanol was heated on the oil-bath at 80 °C for 5 min. The reaction was monitored by TLC. On completion (monitored by TLC), the reaction mixture was diluted with EtOAc (10 mL) and filtered to separate cellulose [2-(sulfooxy)ethyl]mercaptosulfonic acid[SEMSA] from reaction mixture. The filtrate was washed with distilled water and dried over anhydrous Na_2SO_4. Finally, the product was obtained after removal of solvent under reduced pressure followed by crystallization from EtOAc: pet ether. The catalyst was washed with EtOAc (2 × 5 mL) followed by double distilled water (2 × 10 mL). It was dried for 2 h and then reused for subsequent reactions.

Spectral data analysis of the synthesized compounds

3,3,6,6-Tetramethyl-9-phenyl-1,8-dioxodecahydroacridine **(6a)** White-colored solid; M.Pt. 275–276 °C (Lit. M.Pt. 277–278 °C) [96]; ^{1}H NMR (400 MHz, DMSO-d_6): δ 1.05 (s, 6H, 2 × CH_3), 1.19 (s, 6H, 2 × CH_3), 2.23–2.56 (m, 8H, 4 × CH_2), 6.07 (s, 1H, CH), 7.27–7.59 (m, 5H, ArH), 11.62 (bs, 1H, NH);^{13}C NMR (100 MHz, DMSO-d_6): δ 27.6, 28.9, 30.9, 31.7, 46.1, 46.7, 114.9, 127.8, 131.2, 135.4, 149.5, 190.0.

3,3,6,6-Tetramethyl-9-(4-methoxyphenyl)-1,8-dioxodecahydroacridin **(6b)** Yellow-colored crystals; M.Pt. 268–271 °C (Lit. M.Pt. 272–273 °C) [96]; ^{1}H NMR (400 MHz, DMSO-d_6): δ 0.87 (s, 6H, 2 × CH_3), 1.01 (s, 6H, 2 × CH_3), 1.96–2.00 (d, 2H, J = 16 Hz, CH_2), 2.15–2.19 (d, 2H, J = 16 Hz, CH_2), 2.29–2.33 (d, 2H, J = 16 Hz, CH_2), 2.42–2.46 (d, 2H, J = 16 Hz, CH_2), 3.66 (s, 3H, OCH_3), 4.74 (s, 1H, CH), 6.70–6.72 (d, 2H, J = 8 Hz, ArH), 7.04–7.06 (d, 2H, J = 8 Hz, ArH), 9.28 (bs, 1H, NH);^{13}C NMR (100 MHz, DMSO-d_6): δ 27.1, 29.4, 32.4, 40.0, 50.7, 55.4, 112.5, 113.5, 129.2, 139.8, 149.8, 157.5, 195.2.

3,3,6,6-Tetramethyl-9-(4-N,N-dimethylphenyl)-1,8-dioxodecahydroacridine **(6c)** Orange-colored crystals; M.Pt. 264–265 °C (Lit. M.Pt. 265–267 °C) [96]; ^{1}H NMR (400 MHz, DMSO-d_6): δ 0.88 (s, 6H, 2 × CH_3), 1.01 (s, 6H, 2 × CH_3), 1.95–1.99 (d, 2H, J = 16 Hz, CH_2), 2.14–2.18 (d, 2H, J = 16 Hz, CH_2), 2.28–2.32 (d, 2H, J = 16 Hz, CH_2), 2.41–2.45 (d, 2H, J = 16 Hz, CH_2), 2.79 (s, 6H, CH_3), 4.68 (s, 1H, CH), 6.51–6.53 (d, 2H, J = 8 Hz, ArH), 6.94–6.97 (d, 2H, J = 12 Hz, ArH), 9.22 (bs, 1H, NH)^{13}C NMR (100 MHz, DMSO-d_6): δ 29.3, 28.2, 33.5, 35.6, 46.0, 47.8, 114.0, 126.7, 133.5, 136.7, 146.6, 150.5, 191.8.

3,3,6,6-Tetramethyl-9-(3-nitrophenyl)-1,8-dioxodecahydroacridne **(6d)** Yellow-colored crystals; M.Pt. 266–288 °C (Lit. M.Pt. 287–289 °C) [96]; ^{1}H NMR (400 MHz, DMSO-d_6): δ 1.15 (s, 6H, 2 × CH_3), 1.30 (s, 6H, 2 × CH_3), 2.38–2.50 (m, 8H, 4 × CH_2), 5.57 (s, 1H, CH), 7.29–8.08 (m, 4H, ArH), 11.89 (bs, 1H, NH);^{13}C NMR (100 MHz, DMSO-d_6): δ 27.0, 29.3, 31.3, 32.8, 42.9, 46.4, 114.8, 119.5, 121.06, 122.2, 129.1, 133.0, 140.3, 148.5, 191.0.

3,3,6,6-Tetramethyl-9-(4-chlorophenyl)-1,8-dioxodecahydroacridine **(6e)** White-colored solid; M.Pt. 290–294 °C (Lit. M.Pt. 294–296 °C) [96]; ^{1}H NMR (400 MHz, DMSO-d_6): δ 0.90 (s, 6H, 2 × CH_3), 1.04 (s, 6H, 2 × CH_3), 2.06–2.10 (d, 2H, J = 16 Hz, CH_2), 2.25–2.29 (d, 2H, J = 16 Hz, CH_2), 2.49–2.60 (m, 4H, CH_2), 4.49 (s, 1H, CH), 7.17–7.19 (d, 2H, J = 8 Hz, ArH), 7.27–7.29 (d, 2H, J = 8 Hz, ArH), 9.35 (bs, 1H, NH);^{13}C NMR (100 MHz, DMSO-d_6): δ 27.1, 29.1, 31.4, 32.1, 50.4, 114.4, 128.5, 130.4, 131.1, 143.5, 163.8, 196.8.

3,3,6,6-Tetramethyl-9,10-diphenyl-1,8-dioxodecahydroacridine **(7a)** Yellow solid; M.Pt. 250–252 °C (Lit. M.P. 253–255 °C) [97]; ^{1}H NMR (400 MHz, DMSO-d_6): δ 0.85 (s, 6H, 2 × CH_3), 1.01 (s, 6H, 2 × CH_3), 1.83–2.49 (m, 8H, 4 × CH_2), 4.83 (s, 1H, CH), 7.02–7.16 (m, 5H, ArH), 7.27–7.32 (m, 5H, ArH);^{13}C NMR (100 MHz, DMSO-d_6): δ 27.2, 28.3, 40.5, 40.9, 51.3, 111.9, 116.3, 118.8, 125.8, 128.7, 129.1, 129.6, 141.3, 142.2, 153.3, 198.9.

3,3,6,6-Tetramethyl-9-(4-methoxyphenyl)-10-(4-chlorophenyl)-1,8-dioxodecahydroacridine **(7b)** Yellow-colored crystals; M.Pt. 254–255 °C; (Lit. M.Pt. 255–257 °C) [77]; ^{1}H NMR (400 MHz, DMSO-d_6): δ 0.72 (s, 6H, 2 × CH_3), 0.89 (s, 6H, 2 × CH_3), 1.74–1.78 (d, 2H, J = 16 Hz, CH_2), 1.98–2.02 (d, 2H, J = 16 Hz, CH_2), 2.16–2.21 (m, 4H, 2 × CH_2), 3.69 (s, 3H, OCH_3), 4.96 (s, 1H, CH), 6.79–6.81 (d, 3H, J = 8 Hz, ArH), 7.19–7.21 (d, 3H, J = 8 Hz, ArH),

7.67–7.69 (d, 2H, J = 8 Hz, ArH);^{13}C NMR (100 MHz, DMSO-d_6): δ 26.4, 29.8, 32.1, 32.4, 41.4, 50.1, 113.1, 117.4, 128.5, 130.1, 130.8, 139.1, 145.8, 151.1, 156.8, 195.9.

***3,3,6,6-Tetramethyl-9-(4-chlorophenyl)-10-(4-fluorophenyl)-1,8-dioxodecahydroacridine* (7c)** Yellow-colored crystals; M.P. 278–280 °C; ^{1}H NMR (400 MHz, DMSO-d_6): δ 0.72 (s, 6H, 2 × CH_3), 0.89 (s, 6H, 2 × CH_3), 1.75–1.79 (d, 2H, J = 16 Hz, CH_2), 1.99–2.03 (d, 2H, J = 16 Hz, CH_2), 2.17 (s, 2H, CH_2), 2.21–2.22 (d, 2H, J = 4 Hz, CH_2), 5.01 (s, 1H, CH), 7.29–7.33 (m, 4H, ArH), 7.43–7.47 (m, 4H, ArH);^{13}C NMR (100 MHz, DMSO-d_6): δ 26.4, 29.1, 31.4, 32.4, 41.4, 50.0, 55.1, 113.5, 113.8, 128.8, 130.4, 134.5, 137.5, 138.8, 150.8, 157.8, 196.2.

***3,3,6,6-Tetramethyl-9-(4-chlorophenyl)-10-phenyl-1,8-dioxodecahydroacridine* (7d)** White-colored solid; M.P. 240–244 °C; (Lit. M.P. 244–246 °C) [94]; ^{1}H NMR (400 MHz, DMSO-d_6): δ 0.83 (s, 6H, 2 × CH_3), 0.95 (s, 6H, 2 × CH_3), 1.80–2.23 (m, 8H, 4 × CH_2), 5.21 (s, 1H, CH), 7.22–7.27 (m, 4H, ArH), 7.38–7.58 (m, 5H, ArH);^{13}C NMR (100 MHz, DMSO-d_6): δ 26.7, 29.5, 32.3, 38.1, 41.8, 50.1, 114.1, 115.3, 119.3, 128.1, 129.4, 129.7, 131.3, 138.8, 144.6, 149.8, 195.5.

***3,3,6,6-Tetramethyl-9-(4-nitrophenyl)-10-(4-chlorophenyl)-1,8-dioxodecahydroacridine* (7e)** Yellow-colored solid; M.P. 270–272 °C(Lit. M.P. 315–316 °C [95]; ^{1}H NMR (400 MHz, DMSO-d_6): δ 0.71 (s, 6H, 2 × CH_3), 0.90 (s, 6H, 2 × CH_3), 1.78–1.82 (d, 2H, J = 16 Hz, CH_2), 1.99–2.03 (d, 2H, J = 16 Hz, CH_2), 2.19 (s, 2H, CH_2), 2.23–2.24 (d, 2H, J = 4 Hz, CH_2), 5.15 (s, 1H, CH), 7.55–7.60 (m, 4H, ArH), 7.69–7.71 (d, 2H, J = 8 Hz, ArH), 8.14–8.16 (d, 2H, J = 8 Hz, ArH); ^{13}C NMR (100 MHz, DMSO-d_6): δ 26.8, 29.5, 32.7, 33.8, 41.5, 50.3, 112.4, 116.0, 124.1, 129.7, 137.7, 146.5, 151.7, 153.9, 164.8, 196.0.

General procedure for the synthesis of 1,8-dioxo-octahydroxanthenes

To a mixture of aldehyde (1 mmol) and C–H-activated compound (dimedone) and cellulose [2-(sulfooxy)ethyl] mercaptosulfonic acid [SEMSA] (0.1 g) in a round-bottom flask, water (5 mL) was added and the reaction mixture was stirred at 100 °C in case of synthesis of 1,8-dioxo-octahydroxanthenes for an appropriate time. After completion of the reaction (monitored by TLC), the reaction mixture was extracted with hot EtOAc (5–10 mL) and filtered. The organic layer was washed with water and dried over anhyd. Na_2SO_4. Finally, the product was obtained after removal of the solvent under reduced pressure followed by crystallization with EtOAc: pet.ether.

Spectral data of the synthesized compounds

***2,2′-(Phenylmethylene)bis(3-hydroxy-5,5′-dimethyl-2-cyclohexen-1-one)* (12a)** White-colored solid; M.P. 188–190 °C (Lit. M.P. 192–194 °C) [98]; ^{1}H NMR ($CDCl_3$) δ: 1.01 (s, 6H, 2 × –CH_3), 1.14 (s, 6H, 2 × –CH_3), 2.22–2.44 (m, 8H, 4 × -CH_2), 5.49 (s, 1H, -CH), 6.78–7.80 (2H, Ar), 6.92–7.00 (2H, Ar), 11.75 (s, 1H, -OH);^{13}C NMR ($CDCl_3$) δ: 27.32, 29.25, 31.80, 32.2, 40.85, 50.72, 115.66, 126.36, 128.37, 144.0, 162.28, 196.30.

***2,2′-(4-Methoxyphenylmethylene)bis(3-hydroxy-5,5′-dimethyl-2-cyclohexen-1-one)* (12b)** White-colored solid; M.P. 145–147 °C (Lit. M.P. 146–148 °C) [98]; ^{1}H NMR ($CDCl_3$) δ: 1.02 (s, 6H, 2 × –CH_3), 1.12 (s, 6H, 2 × –CH_3), 2.22–2.43 (m, 8H, 4 × –CH_2), 3.45 (s, 3H, -OCH_3), 5.50 (s, 1H, CH), 6.78–7.84 (2H, Ar), 6.92–7.00 (2H, Ar), 11.79 (s, 1H, -OH);^{13}C NMR ($CDCl_3$) δ: 28.33, 29.20, 31.82, 32.2, 40.85, 50.74, 115.60, 126.36, 128.04, 128.35, 144.08, 162.24, 196.30.

***2,2′-(2-Nitrophenylmethylene)bis(3-hydroxy-5,5′-dimethyl-2-cyclohexen-1-one)* (12c)** White-colored solid; M.P. 255–259 °C (Lit. M.P. 258–262 °C) [99];^{1}H NMR ($CDCl_3$) δ ppm: 1.10 (s, 6H, 2 × –CH_3), 1.21 (s, 6H, 2 × –CH_3), 2.24–2.49 (m, 8H, 4 × –CH_2), 5.50 (s, 1H, -CH), 7.06–7.15 (m, 4H, Ar), 11.70 (s, 1H, -OH); ^{13}C NMR ($CDCl_3$) δ ppm: 27.33, 29.30, 31.79, 32.2, 40.90, 50.75, 115.69, 126.40, 128.04, 128.32, 144.08, 163.24, 196.40.

***2,2′-(4-Nitrophenylmethylene)bis(3-hydroxy-5,5′-dimethyl-2-cyclohexen-1-one)* (12d)** Creamish-colored solid; M.P. 192–194 °C (Lit. M.P. 195–197 °C) [99];^{1}H NMR ($CDCl_3$) δ: 1.09 (s, 6H, 2 × –CH_3), 1.20 (s, 6H, 2 × –CH_3), 2.24–2.47 (m, 8H, 4 × –CH_2), 5.52 (s, 1H, -CH), 7.06–7.17 (m, 4H, Ar), 11.77 (s, 1H, -OH);^{13}C NMR ($CDCl_3$) δ: 27.39, 29.20, 31.86, 32.2, 40.88, 50.64, 115.56, 126.29, 128.04, 128.37, 144.08, 164.24, 195.33.

***2,2′-(4-Bromophenylmethylene)bis(3-hydroxy-5,5′-dimethyl-2-cyclohexen-1-one)* (12e)** White-colored solid; M.Pt. 150 °C); ^{1}H NMR ($CDCl_3$) δ: 1.05 (s, 6H, 2 × –CH_3), 1.19 (s, 6H, 2 × –CH_3), 2.20–2.39 (m, 8H, 4 × –CH_2), 5.32 (s, 1H, -CH), 7.18–7.20 (m, 4H, Ar), 11.71 (s, 1H, -OH); ^{13}C NMR($CDCl_3$) δ: 27.35, 29.29, 31.80, 32.2, 40.85, 50.79, 115.60, 126.33, 128.00, 128.38, 144.08, 162.29, 196.34.

***2,2′-(3-Nitrophenylmethylene)bis(3-hydroxy-5,5′-dimethyl-2-cyclohexen-1-one)* (12f)** Creamish-colored solid; M.Pt. 200 °C (Lit. M.Pt. 201–203 °C) [98]; ^{1}H NMR ($CDCl_3$) δ: 1.07 (s, 6H, 2 × –CH_3), 1.22 (s, 6H, 2 × –CH_3), 2.24–2.44 (m, 8H, 4 × –CH_2), 5.52 (s, 1H, -CH), 7.06–7.18 (m, 4H, Ar), 11.79 (s, 1H, -OH); ^{13}C NMR($CDCl_3$) δ: 27.33, 29.30,

31.75, 32.78, 40.77, 50.74, 115.64, 126.80, 128.0, 128.37, 145.08, 162.20, 196.28.

2,2'-(2-Bromophenylmethylene)bis(3-hydroxy-5,5'-dimethyl-2-cyclohexen-1-one) **(12g)** White-colored solid; M.Pt. 238–240 °C (Lit. M.Pt. 241–243 °C) [98]; ^{1}H NMR ($CDCl_3$) δ: 1.01 (s, 6H, 2×–CH_3), 1.12 (s, 6H, 2×–CH_3), 2.19–2.34 (m, 8H, 4×–CH_2), 5.43 (s, 1H, -CH), 6.90–6.98 (m, 4H, Ar), 11.82 (s, 1H, -OH); ^{13}C NMR($CDCl_3$) δ: 26.72, 29.37, 31.79, 32.20, 42.87, 51.75, 115.57, 126.30, 128.6, 128.37, 144.08, 162.27, 196.47.

2,2'-(2-Chlorophenylmethylene)bis(3-hydroxy-5,5'-dimethyl-2-cyclohexen-1-one) **(12h)** Creamish-colored solid; M.Pt. 202–204 °C (Lit. M.Pt. 202–204 °C) [98]; ^{1}H NMR ($CDCl_3$) δ: 1.05 (s, 6H, 2×–CH_3), 1.14 (s, 6H, 2×–CH_3), 2.19–2.36 (m, 8H, 4×–CH_2), 5.47 (s, 1H, -CH), 6.90–6.95 (m, 4H, Ar), 11.80 (s, 1H, -OH); ^{13}C NMR($CDCl_3$) δ: 26.99, 28.27, 31.78, 32.2, 43.87, 52.74, 115.67, 125.36, 127.04, 128.37, 142.08, 162.29, 196.29.

2,2'-(4-Chlorophenylmethylene)bis(3-hydroxy-5,5'-dimethyl-2-cyclohexen-1-one) **(12i)** Creamish-colored solid; M.Pt. 145–148 °C (Lit. M.Pt. 145–147 °C) [98]; ^{1}H NMR ($CDCl_3$) δ: 1.00 (s, 6H, 2×–CH_3), 1.10 (s, 6H, 2×–CH_3), 2.19–2.35 (m, 8H, 4×–CH_2), 5.45 (s, 1H, -CH), 6.90–6.97 (m, 4H, Ar), 11.80 (s, 1H, -OH); ^{13}C NMR($CDCl_3$) δ: 27.33, 29.27, 31.83, 32.2, 40.87, 50.74, 115.67, 126.36, 128.04, 128.37, 144.08, 162.24, 196.3.

2,2'-(4-Methylphenylmethylene)bis(3-hydroxy-5,5'-dimethyl-2-cyclohexen-1-one) **(12j)** White-colored solid; M.Pt. 138–140 °C (Lit. M.Pt. 141–143 °C) [98]; ^{1}H NMR ($CDCl_3$) δ: 1.02 (s, 6H, 2×–CH_3), 1.15 (s, 6H, 2×–CH_3), 2.19 (s, 3H, -CH_3) 2.36–2.57 (m, 8H, 4×–CH_2), 5.62 (s, 1H, -CH), 6.80–6.89 (2H, Ar), 6.90–7.19 (2H, Ar), 11.84 (s, 1H, -OH); ^{13}C NMR($CDCl_3$) δ: 27.30, 29.29, 31.81, 32.29, 46.87, 50.70, 115.72, 126.45, 128.12, 128.37, 144.25, 162.28, 195.32.

9-Phenyl-1,8-dioxo-octahydroxanthene **(13a)** White-colored solid; M.Pt. 202 °C (Lit. M.Pt. 205 °C) [98]; ^{1}H NMR ($CDCl_3$) δ: 0.99 (s, 6H, 2×–CH_3), 1.12 (s, 6H, 2×–CH_3), 2.14–2.47 (m, 8H, 4×–CH_2), 4.53 (s, 1H, -CH), 7.07–7.27 (m, 5H, Ar); ^{13}C NMR($CDCl_3$) δ: 27.33, 29.27, 31.83, 32.2, 40.87, 50.74, 115.67, 126.36, 128.04, 128.37, 144.08, 162.24, 196.3.

9-(4'-Methoxyphenyl)-1,8-dioxo-octahydroxanthene **(13b)** White-colored solid; M.Pt. 238–240 °C (Lit. M.Pt. 242–243 °C) [98]; ^{1}H NMR ($CDCl_3$) δ: 1.08 (s, 6H, 2×–CH_3), 1.21 (s, 6H, 2×–CH_3), 2.27–2.37 (m, 8H, 4×–CH_2), 3.49 (s, 3H, -OCH_3), 4.53 (s, 1H, -CH), 6.78–6.80 (d, 2H, Ar), 7.22–7.24 (d, 2H, Ar); ^{13}C NMR($CDCl_3$) δ: 27.39, 29.27, 31.40, 32.05, 46.47, 47.4, 113.67, 115.02, 127.36, 129.04, 157.37, 189.08, 190.24.

9-(2'-Nitrophenyl)-1,8-dioxo-octahydroxanthene **(13c)** White-colored solid;M.Pt. 248–250 °C (Lit. M.Pt. 252–254 °C) [98]; ^{1}H NMR ($CDCl_3$) δ: 1.16 (s, 6H, 2×–CH_3), 1.25 (s, 6H, 2×–CH_3), 2.37–2.59 (m, 8H, 4×–CH_2), 4.86 (s, 1H, -CH), 7.29 (d, 2H, Ar), 8.15 (d, 2H, Ar); ^{13}C NMR($CDCl_3$) δ: 27.15, 29.50, 32.69, 50.14, 56.80, 60.20, 105.20, 115.15, 136.78, 140.80, 153.70, 163.83, 197.19.

9-(4'-Nitrophenyl)-1,8-dioxo-octahydroxanthene **(13d)** White-colored solid; M.Pt. 220–222 °C (Lit. M.Pt. 222–224 °C) [98]; ^{1}H NMR ($CDCl_3$) δ: 1.19 (s, 6H, 2×–CH_3), 1.24 (s, 6H, 2×–CH_3), 2.37–2.57 (m, 8H, 4×–CH_2), 4.86 (s, 1H, -CH), 7.27 (d, 2H, Ar), 8.14 (d, 2H, Ar); ^{13}C NMR($CDCl_3$) δ: 27.14, 29.60, 32.72, 50.16, 56.85, 60.19, 106.20, 115.10, 136.85, 140.78, 153.68, 163.93, 197.17.

9-(4'-Bromophenyl)-1,8-dioxo-octahydroxanthene **(13e)** White-colored solid; M.Pt. 238–240 °C (Lit. M.Pt. 240–242 °C) [98]; ^{1}H NMR ($CDCl_3$) δ: 1.10 (s, 6H, 2×–CH_3), 1.23 (s, 6H, 2×–CH_3), 2.37–2.57 (m, 8H, 4×–CH_2), 4.86 (s, 1H, -CH), 7.27 (d, 2H, Ar), 8.15 (d, 2H, Ar); ^{13}C NMR($CDCl_3$) δ: 27.14, 29.56, 32.70, 50.14, 56.88, 60.10, 106.18, 115.15, 136.85, 140.78, 153.68, 163.83, 197.10.

9-(3'-Nitrophenyl)-1,8-dioxo-octahydroxanthene **(13f)** White-colored solid; M.Pt. 162–165 °C (Lit. M.Pt. 165–166 °C) [98]; ^{1}H NMR ($CDCl_3$) δ: 1.18 (s, 6H, 2×–CH_3), 1.23 (s, 6H, 2×–CH_3), 2.37–2.57 (m, 8H, 4×–CH_2), 4.86 (s, 1H, -CH), 7.26 (d, 2H, Ar), 8.14 (d, 2H, Ar); ^{13}C NMR($CDCl_3$) δ: 27.14, 29.60, 32.75, 50.16, 56.83, 60.19, 106.24, 115.10, 136.85, 140.78, 153.68, 163.93, 197.17.

9-(2'-Bromophenyl)-1,8-dioxo-octahydroxanthene **(13g)** White-colored solid;M.Pt. 222–224 °C (Lit. M.Pt. 226–229 °C) [98]; ^{1}H NMR ($CDCl_3$) δ: 1.10 (s, 6H, 2×–CH_3), 1.28 (s, 6H, 2×–CH_3), 2.37–2.58 (m, 8H, 4×–CH_2), 4.86 (s, 1H, -CH), 7.25 (d, 2H, Ar), 8.10 (d, 2H, Ar); ^{13}C NMR($CDCl_3$) δ: 27.14, 29.58, 32.79, 50.10, 56.83, 60.19, 106.27, 115.12, 136.84, 140.78, 153.70, 163.93, 197.19.

9-(2'-Chlorophenyl)-1,8-dioxo-octahydroxanthene **(13h)** White-colored solid;M.Pt. 225 °C (Lit. M.Pt. 226–227 °C) [98]; ^{1}H NMR ($CDCl_3$) δ: 1.08 (s, 6H, 2×–CH_3), 1.20 (s, 6H, 2×–CH_3), 2.27–2.47 (m, 8H, 4×–CH_2), 4.51 (s, 1H, -CH), 6.90–7.0 (d, 2H, Ar), 7.22–7.24 (d, 2H, Ar); ^{13}C NMR($CDCl_3$) δ: 27.70, 29.72, 31.80, 32.60, 41.37, 51.11, 115.60, 128.60, 130.20, 132.40, 143.11, 162.80, 196.70.

9-(4'-Chlorophenyl)-1,8-dioxo-octahydroxanthene **(13i)** White-colored solid;M.Pt. 229–231 °C (Lit. M.Pt.

230–232 °C) [98]; ^{1}H NMR ($CDCl_3$) δ: 1.08 (s, 6H, 2×–CH_3), 1.22 (s, 6H, 2×–CH_3), 2.27–2.47 (m, 8H, 4 x vCH_2), 4.51 (s, 1H, -CH), 6.90–7.4 (d, 2H, Ar), 7.22–7.26 (d, 2H, Ar); ^{13}C NMR($CDCl_3$) δ: 27.70, 29.75, 31.83, 32.60, 41.31, 51.61, 115.62, 128.69, 130.25, 132.40, 143.17, 162.80, 196.75.

***9-(4'-Methylphenyl)-1,8-dioxo-octahydroxanthene* (13j)** White-colored solid;M.Pt. 212–215 °C (Lit. M.Pt. 215–216 °C) [98]; ^{1}H NMR ($CDCl_3$) δ: 0.99 (s, 6H, 2×–CH_3), 1.09 (s, 6H, 2×–CH_3), 2.14–2.20 (d, 4H,), 2.24(s, 3H), 2.45(s, 4H), 4.78 (s, 1H, CH), 6.77–7.27 (4H, Ar); ^{13}C NMR($CDCl_3$) δ: 27.68, 29.70, 31.83, 32.66, 41.31, 51.61, 114.55, 128.60, 130.22, 132.40, 143.01, 162.73, 196.79.

Results and discussion

Characterization of catalyst cellulose[2-(sulfooxy) ethyl]mercaptosulfonic acid[SEMSA]

Fourier transform infrared spectroscopy (FTIR)

The FTIR study of cellulose showed O–H stertching at 3340.85 cm^{-1} and C–H stretching at 2902.03 cm^{-1}. The peak at 1651.14 cm^{-1} showed the bending mode of H_2O, and O–H bending in cellulose shows peak at 1317.44 cm^{-1}. C–O bending in cellulose showed peak at 1160.23 cm^{-1} as shown in Fig. 2. The FTIR spectral studies of cellulose sulfonic acid showed absorption peaks at 3341.82 cm^{-1} due to O–H stretching. The peak at 1109.12 cm^{-1} was shown due to C–O stretching, and peak at 1058.00 cm^{-1} was due to C–C vibration. C–H ring stretching showed peak at 897.90 cm^{-1}. The peak at 1160.23 cm^{-1} was due to O=S=O asymmetric stretching vibration of sulfonic acid groups. The peak shown at 1034.85 cm^{-1} was due to O=S=O symmetric stretching vibration of sulfonic acid groups and a peak at 665.47 cm^{-1} was due to S–O stretching vibration of sulfonic groups as shown in Fig. 3.

The FTIR spectral studies of (Fig. 4) cellulose[2-(sulfooxy) ethyl]mercaptosulfonic acid[SEMSA] showed absorption peaks at 663 cm^{-1} due to C–S stretching vibration. A peak at 898 cm^{-1} was observed due to C–O–C stretching at β-(1,4)-glycosidic linkages. 1283, 1157 and 1069 cm^{-1} was attributed to asymmetric stretching of –SO_2 moieties. 2902 cm^{-1} was due to C–H stretching vibration and 3340 cm^{-1} due to -OH stretching vibration. This catalyst showed absorption peaks at 886, 852 cm^{-1} due to S–OH bending and 613, 590 cm^{-1} peaks observed due to S–O symmetric stretching confirming the formation of the desired catalyst.

Thermo-gravimetric analysis (TGA)

Thermal stability of cellulose–sulfonic acid was determined with thermo-gravimetric analysis (TGA). The curve showed an initial weight loss of 3.4% up to 185.85 °C which may be due to the loss of residual water trapped onto the surface of cellulose sulfonic acid and then a weight loss of 7.52% up to 342.58 °C followed by continuous weight loss up to 875.44 °C. From the observed data, it is confirmed that the catalyst is stable up to 185 °C and thus is safe to carry out the reaction for the chosen conditions, i.e. room temperature and 185 °C (Fig. 5).

Thermal stability of the cellulose[2-(sulfooxy)ethyl]mercaptosulfonic acid was determined using thermo-gravimetric

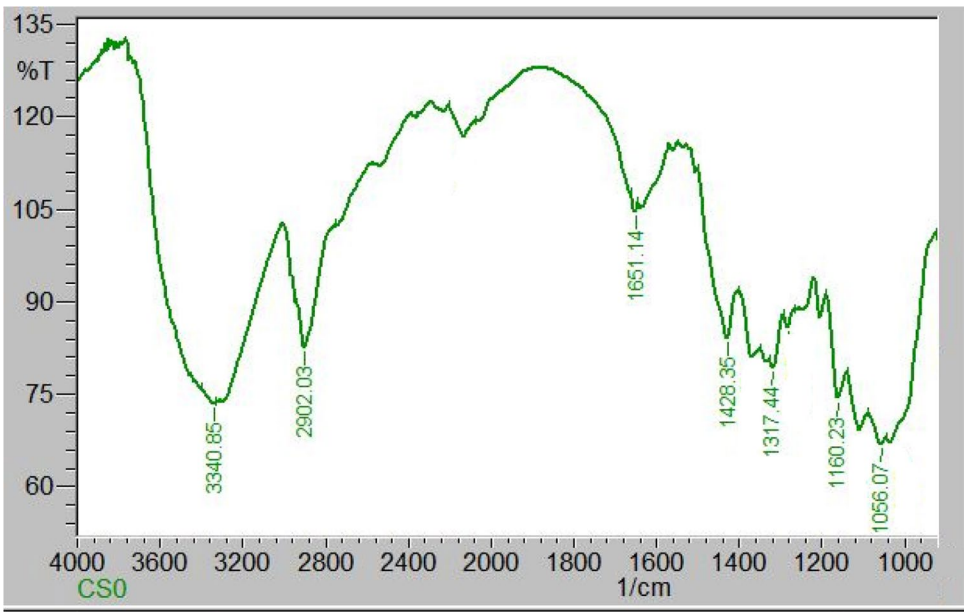

Fig. 2 FTIR Spectra of cellulose

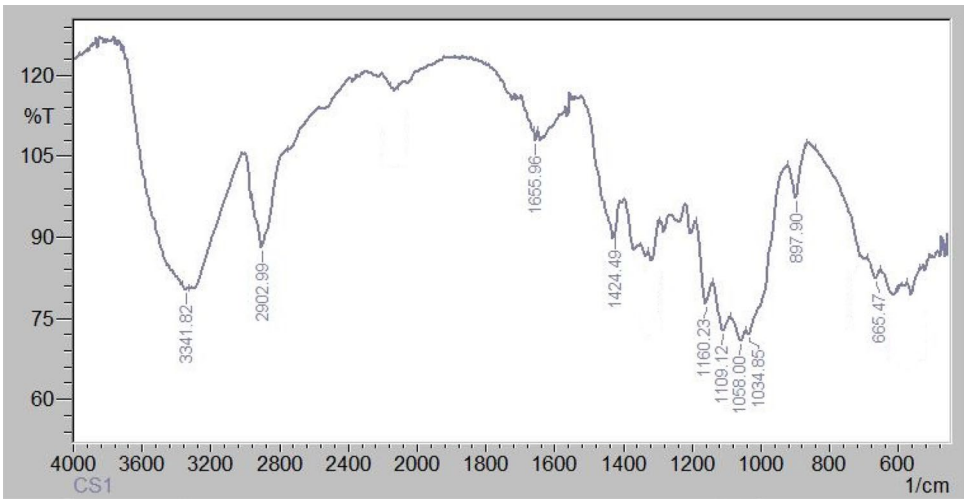

Fig. 3 FTIR Spectra of [cellulose-SO_3H]

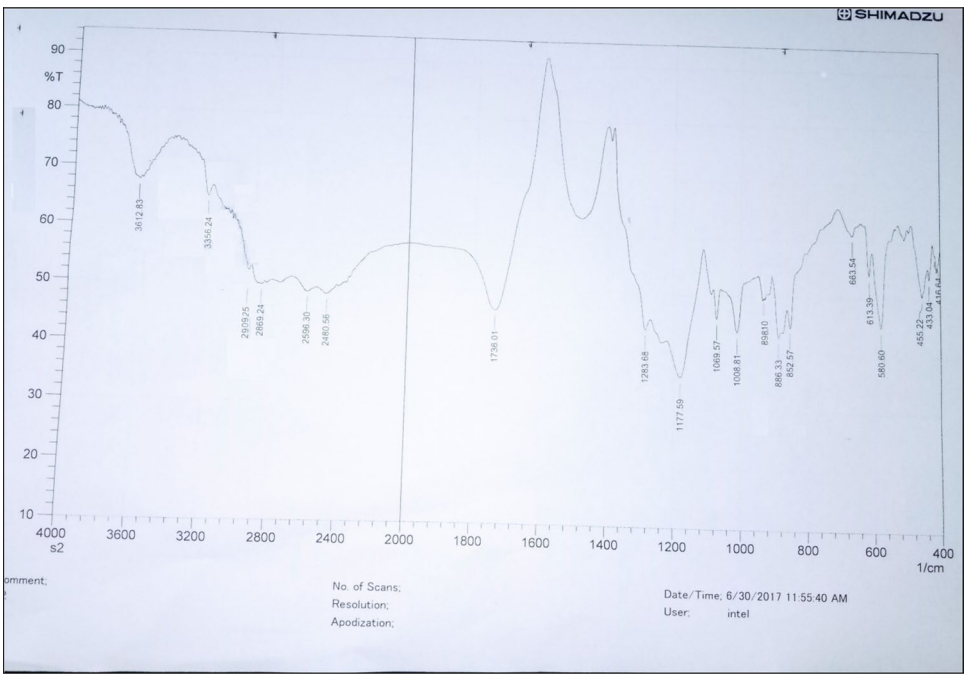

Fig. 4 FTIR of nanocatalyst, i.e. cellulose[2-(sulfooxy)ethyl]mercaptosulfonic acid[SEMSA]

analysis (TGA). The curve showed an initial weight loss of 1.997% up to 50.57 °C which may be due to the loss of residual water trapped onto the surface of cellulose sulfonic acid and then a weight loss of 6.088% up to 153.68 °C followed by continuous weight loss up to 898 °C. Thus, from the TGA analysis, it can be confirmed that the catalyst is stable up to 898 °C, concluded that it could be safely used in organic reactions below 898 °C (Fig. 6).

Scanning electron microscopy (SEM)

The topography of the cellulose[2-(sulfooxy)ethyl]mercaptosulfonic acid was studied by using a scanning electron microscope (FEG-SEM). (FEG-SEM) micrographs showed the presence of aggregates of particles with somewhat spherical morphology and represents that the catalyst particles showed fibrous surface having very small size (nanometers to micrometers) as shown in Fig. 7a, b.

Transmission electron microscopy (TEM)

The TEM analysis revealed various parameters of the internal morphology and fine structure of carbon-based nanocatalyst. Figure 8a, b showed uniform distribution onto the surface of cellulose and the presence of spherical particles. The TEM images provided average particle size of nanoparticles which was found to be in the range of 17–31.4 nm.

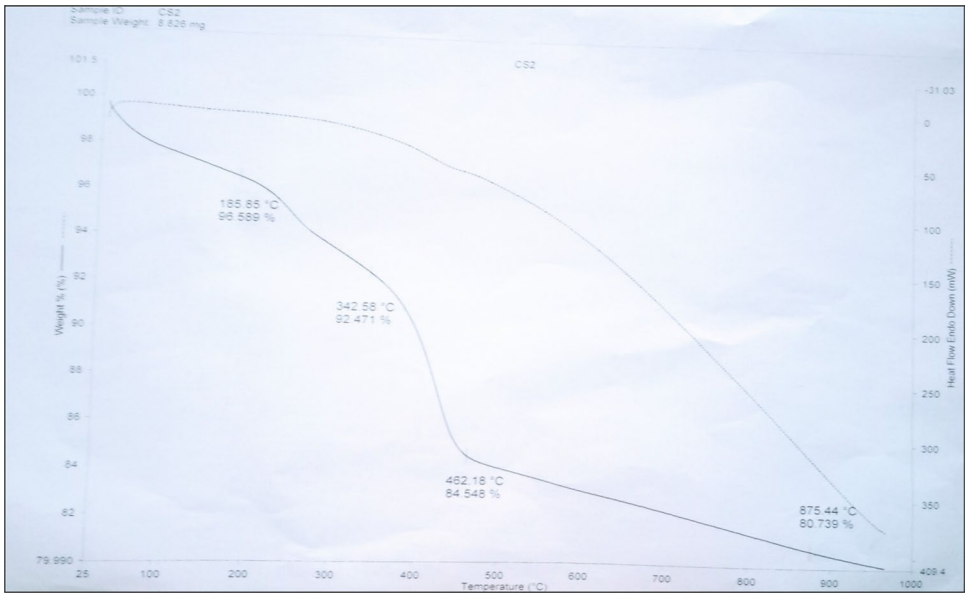

Fig. 5 TGA graph of [cellulose-SO_3H]

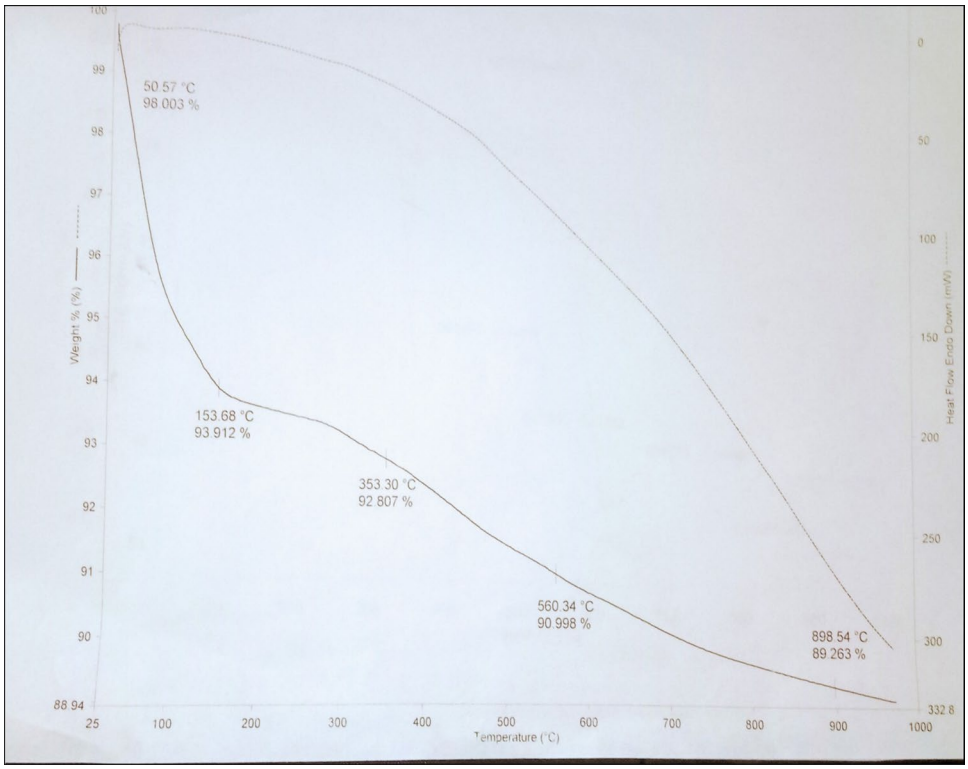

Fig. 6 TGA of nanocatalyst, i.e. cellulose[2-(sulfooxy)ethyl]mercaptosulfonic acid[SEMSA]

High-resolution transmission electron microscopy (HR-TEM)

The sustainability of the catalyst was confirmed by the HR-TEM of the recycled catalyst of 5th cycle. There was aggregation of the catalyst which leads to the formation of rod-shaped structure shown in Fig. 9. The surface area was reduced for the reaction platform, and hence the yield was also slightly reduced for the 6th cycle of reaction.

Testing of catalytic activity of nanocatalyst cellulose[2-(sulfooxy)ethyl]mercaptosulfonic acid[SEMSA]

Catalyst testing for the synthesis of *gem*-bisamides

Our initial efforts were focused on finding the most effective catalyst among the various solid acid catalyst. In

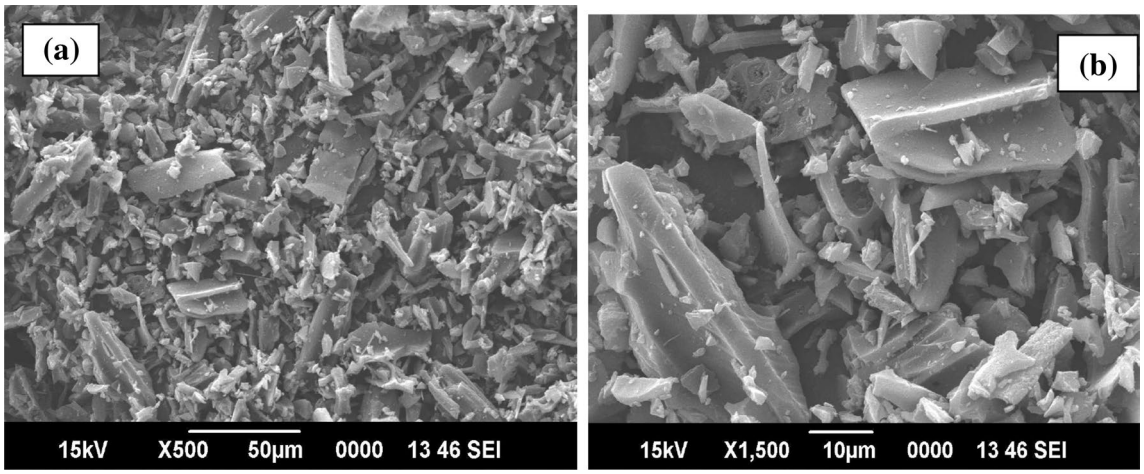

Fig. 7 SEM images of nanocatalyst, i.e. cellulose[2-(sulfooxy)ethyl]mercaptosulfonic acid[SEMSA]

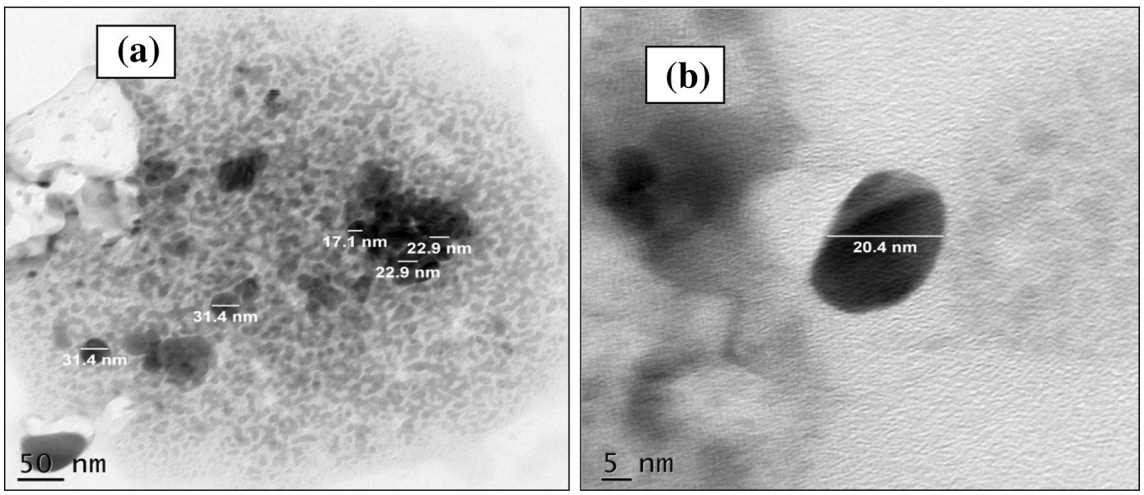

Fig. 8 TEM images of nanocatalyst cellulose[2-(sulfooxy)ethyl]mercaptosulfonic acid[SEMSA]

order to screen the catalysts, the reaction of benzamide and benzaldehyde was taken as a model reaction in the presence of toluene at 110 °C. In order to further make the reaction conditions milder and effective, the test reaction was also attempted with different catalysts such as SiO_2-*p*-TsOH, cellulose-SO_3H, SiO_2-SO_3H [cellulose-SO_3H][BMIM][BF_4] and cellulose[2-(sulfooxy)ethyl] mercaptosulfonic acid[SEMSA]. Among various tried catalysts, it was found that the reaction with nanocatalyst, i.e. cellulose[2-(sulfooxy)ethyl]mercaptosulfonic acid, proceeded efficiently in lesser time giving good yield. Thus, cellulose[2-(sulfooxy)ethyl]mercaptosulfonic acid[SEMSA] was selected as the optimum reaction catalyst at which the reaction proceeded smoothly and gave better yields of products with good selectivity. It was found that among various composites, cellulose[2-(sulfooxy) ethyl]mercaptosulfonic acid[SEMSA] efficiently catalyzed the synthesis of *gem*-bisamides both in terms of reaction time and yield as shown in Table 1. Further, in order to optimize the amount of catalyst, we analyzed the reaction by varying the amount to 0.05 g, 0.08 g, 0.1 g, 0.15 g and 0.5 g cellulose[2-(sulfooxy)ethyl]mercaptosulfonic acid [SEMSA], and the optimum amount of catalyst turns out to be 0.1 g in order to obtain the best results. To study the solvent effect on the reaction of benzamide and benzaldehyde in the presence of nanocatalyst, i.e. cellulose[2-(sulfooxy)ethyl]mercaptosulfonic acid[SEMSA], we carried out the reaction in different solvents such as ethanol, acetonitrile, water, dichloromethane, toluene and solvent-free conditions.

When the reaction was performed in ethanol, acetonitrile and water, only trace amount of product formation

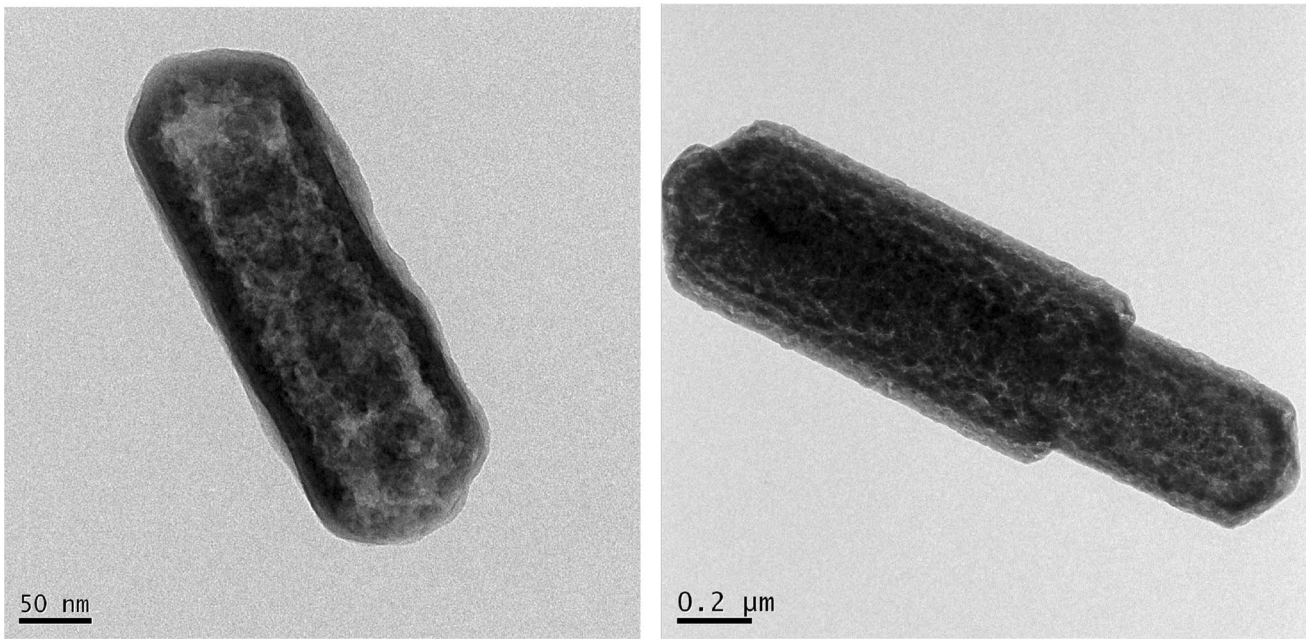

Fig. 9 HR-TEM images of recycled nanocatalyst cellulose[2-(sulfooxy)ethyl]mercaptosulfonic acid[SEMSA]

Table 1 Effect of different solid acid catalysts studied for the synthesis of *gem*-bisamides, hexahydroacridines-1,8-diones and 1,8-dioxo-octahydroxanthenes

gem-bisamides				Hexahydroacridines-1,8-diones		1,8-dioxo-octahydroxanthenes	
Entry	Catalysts	Time (min.)	Yield (%)[a]	Time (min.)	Yield (%)[a]	Time (min.)	Yield (%)[a]
1	SiO_2-*p*-TsOH	300	50	60	55	30	65
2	Cellulose-SO_3H	240	60	50	75	25	70
3	SiO_2-SO_3H	360	45	60	50	20	75
4	Cellulose-SO_3H [BMIM][BF_4]	120	70	40	75	10	80
5	**Nanocatalyst**	**10**	**93**	**10**	**94**	**3**	**94**

[a]Isolated yields

Table 2 Effect of different solvents on cellulose[2-(sulfooxy)ethyl]mercaptosulfonic acid[SEMSA] catalyzed one-pot synthesis of *gem*-bisamides, hexahydroacridines-1,8-diones and 1,8-dioxo-octahydroxanthenes

gem-bisamides[a]					Hexahydroacridines-1,8-diones[b]		1,8-dioxo-octahydroxanthenes[c]	
Entry	Solvents	Temp. (°C)	Time (min.)	Yield (%)[d]	Time (min.)	Yield (%)[d]	Time (min.)	Yield (%)[d]
1	Ethanol	80	240	60	**10**	**94**	10	75
2	Acetonitrile	82	125	55	60	50	**3**	**94**
3	Water	100	–	–	50	75	25	70
4	Toluene	110	**10**	**93**	40	85	–	–
5	Dichloro methane	60	180	30	240	20	20	75
6	Solvent-free	80	120	75	300	ND[d]	30	65

Bold values indicate the optimized reaction conditions

[a]Reaction conditions: aldehyde (1 mmol), dimedone (2 mmol) and catalyst (0.1 g) at 110 °C using toluene (5 mL) as a solvent

[b]Reaction conditions: aldehyde (1 mmol), dimedone (2 mmol), NH_4OAc or aromatic amines (1 mmol), catalyst (0.1 g) at 80 °C in presence of ethanol (5 mL) as a solvent

[c]Reaction conditions: aldehyde (1mmol), dimedone (2 mmol) and catalyst (0.1 g) at 80 °C in acetonitrile (5 mL)

[d]Isolated yields

was observed (Table 2, entries 1, 2, 5 and 6), whereas toluene proves as the best solvent as shown in Table 2, entry 4 at 110 °C, both the yield and reaction time were significantly improved. Further, we have tried this reaction applying different temperatures and found that the best reaction in terms of yield occured at 110 °C. Thus, the optimum conditions selected are: benzamide (2 mmol), aldehyde (1 mmol) and cellulose[2-(sulfooxy)ethyl]mercaptosulfonic acid[SEMSA] (0.1 g) under solvent-free conditions at 100 °C. Tables 3, 4 and 5 have provided the various synthetic methodologies reported earlier and gave comparisons between the earlier found results and the result found in the present work for the synthesis of *gem*-bisamides, hexahydroacridines-1,8-diones and 1,8-dioxo-octahydroxanthenes.

In order to inquire the scope of this novel catalytic method, we investigated various aromatic aldehydes containing either electron-withdrawing or electrondonating groups under the optimized reaction conditions, we have obtained excellent results in terms of yield of the product formation. The results are summarized in Table 6, products (3a–k).

Chemical properties of the nanocatalyst verses their roles on the synthesis of *gem*-bisamides, hexahydroacridines-1,8-diones and 1,8-dioxo-octahyroxanthenes

Nanomaterial-based catalysts are usually heterogeneous catalysts broken up into nanoparticles in order to speed up the catalytic process. An increasing demand of carbonaceous solid acid nanocatalyst containing sulfonic acid groups on the surface is due to the presence of sulfonated carbon nanofibres which are obtained by incomplete carbonization of low-cost natural nanofibrous cellulose followed by sulfonation with sulfuric acid, size of the particles in nanometers, high surface area, large pore volume and large number of hydroxyl and carboxyl groups [115]. The modifications on the surface of nanoparticles is the best way to make a connection between homogeneous and heterogeneous catalysis. These catalysts have an important feature of the recyclability with little bit loss in activity. The main aim of nanocatalyst is to increase the chemical stability of the sulfonic acid-functionalized catalysts under milder conditions. Nanocatalyst exhibits an important role in green synthesis. The preparatory methods of nanocatalysts are environmental friendly, inexpensive and easy to come up with many modifications [116].

To explain the formation of bisamides via the one-pot multi-component reaction, we have proposed a plausible reaction mechanism according to which an aldehyde is attacked by an amide moiety, cellulose[2-(sulfooxy)ethyl] mercaptosulfonic acid[SEMSA] activates the aldehyde to be attacked by the amide to undergo Knoenvenagel condensation to form intermediate (A), after that amide moiety attack the C = N bond which is activated by the catalyst in order to produce the desired product as shown in Scheme 2 in supplementary information (S7).

Table 3 Comparison between the results found in case of *gem*-bisamides and the already published results

Entry	Catalyst	Solvent time (min.)	Yield (%)
1	Hydroxyapatite [100]	Acetonitrile 180	95
2	DES as catalyst (deep eutectic solvent) [101]	DES 20 as solvent	90
3	$ZnCl_2/SiO_2$ [102]	Solvent-free 30	89
4	Nano-$TiCl_4.SiO_2$ [103]	Solvent-free 138	93
5	HPVAC [104]	Solvent-free 25	96
6	**Cellulose[2-(sulfooxy) ethyl]mercaptosulfonic acid**	**Ethanol 10**	**94**

Table 4 Comparison between the results found in case of hexahydroacridine-1,8-diones and the already published results

Entry	Catalyst	Solvent time (min.)	Yield (%)
1	MoO_3/SiO_2 [105]	Solvent-free 15	93
2	Alginic acid [106]	Ethanol 180	98
3	KH_2PO_4 [107]	Aqueous ethanol 360	94
4	*N*-Butylpyridinium heptachlorodialuminate [108]	Ethanol 12	94
5	Catalyst free [109]	DMSO 120	98
6	**Cellulose[2-(sulfooxy) ethyl] mercaptosulfonic acid**	**Toluene 10**	**93**

Table 5 Comparison between the results found in case of 1,8-dioxo-octahydroxanthenes and the already published results

Entry	Catalyst	Solvent time (min.)	Yield (%)
1	Fe/MCM-41 [110]	Solvent-free 20	97
2	Fe_3O_4@SiO_2-SO_3H [111]	Solvent-free 50	98
3	Nano-$Ni_{0.5}Co_{0.5}$ Fe_2O_4 [112]	Ethanol:Water 25	95
4	$Cs_{2.5}$ $H_{0.5}$ $PW_{12}O_{40}$ [113]	Water 30	96
5	$Fe_2(SO_4)_3 \cdot 7H_2O$ [114]	Neat 144	94
6	**Cellulose[2-(sulfooxy) ethyl]mercaptosulfonic acid**	**Acetonitrile 3**	**94**

Catalyst testing and role of nanocatalyst in the synthesis of hexahydroacridine-1,8-diones

A preliminary investigation was carried out using dimedone as the C–H-activated compound, 4-methoxybenzaldehyde

Table 6 Cellulose[2-(sulfooxy)ethyl]mercaptosulfonic acid[SEMSA] catalyzed one-pot synthesis of *gem*-bisamides

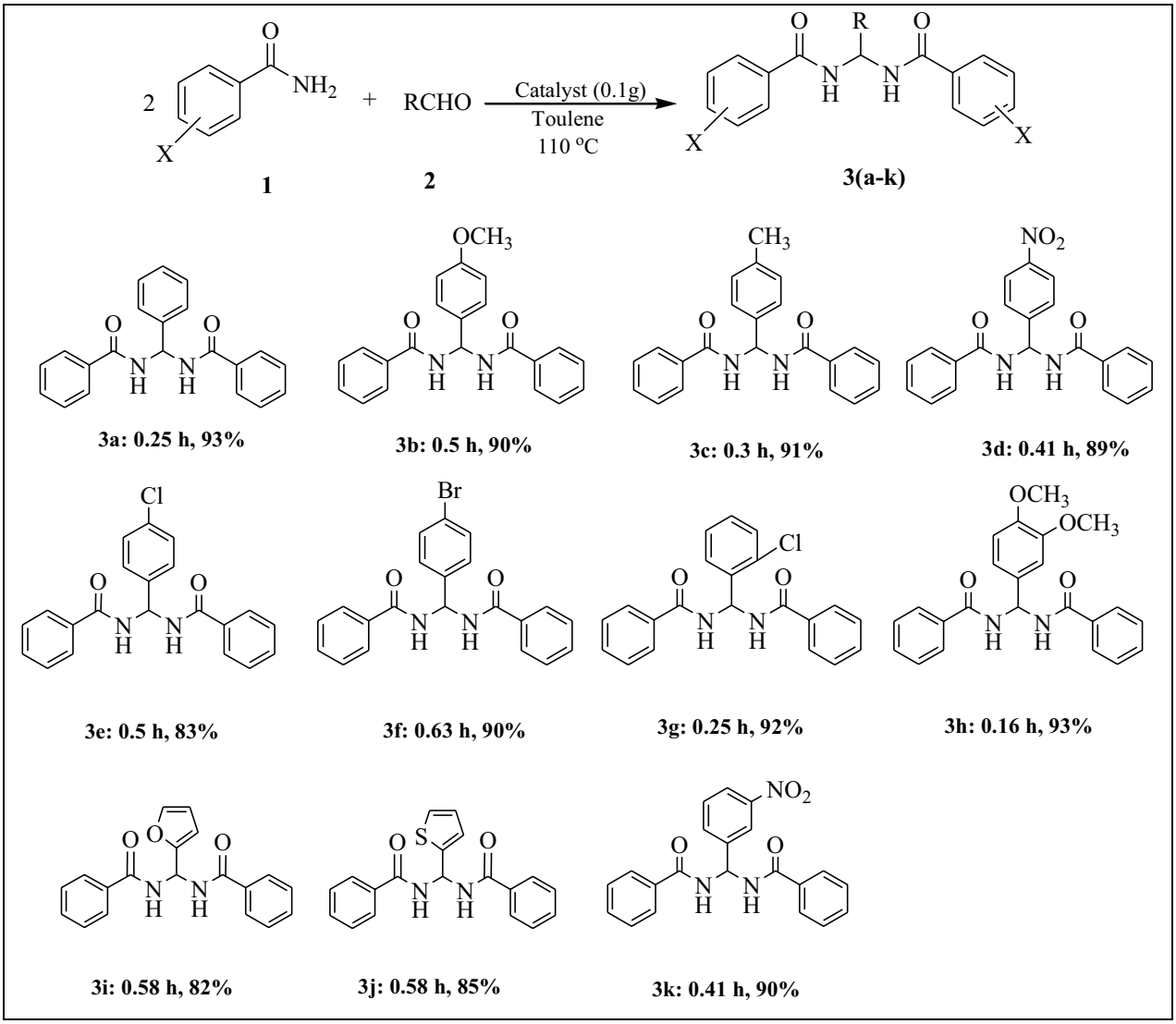

and NH_4OAc as test substrate and it was found that reaction could be finished using catalytic amount of cellulose[2-(sulfooxy)ethyl]mercaptosulfonic acid[SEMSA] and gave desired product in good yield. Different types of catalysts, different amounts of the selected catalyst and different solvents were tried for the best selectivity and found that cellulose[2-(sulfooxy)ethyl]mercaptosulfonic acid[SEMSA] again turned out to be the most active catalyst for the synthesis of acridine derivatives (Table 1, entry 5). Further, 0.1 g of cellulose[2-(sulfooxy)ethyl]mercaptosulfonic acid gave the best results in terms of reaction time and yield and the best solvent comes out to be ethanol (Table 2, entry 1). In order to examine the substrate scope, various aromatic and heteroaromatic aldehydes with different substituents were chosen and excellent results were obtained as shown in Table 7, products (6a–e, 7a–e). The plausible mechanism was suggested for the synthesis of hexahydroacridine-1,8-diones catalyzed by cellulose[2-(sulfooxy)ethyl]mercaptosulfonic acid represented in Scheme 3 of ESM.

Scheme 3 provides the plausible mechanism for the synthesis of hexahydroacridine-1,8-diones catalyzed by cellulose[2-(sulfooxy)ethyl]mercaptosulfonic acid. Firstly this catalyst activates aryl aldehyde and dimedone, which undergo Knoenvenagel condensation to form an intermediate (A). Similarly, another dimedone molecule catalyst reacts with NH_4OAc resulting in the formation of an enamine intermediate (B). (A) and (B) undergoes Michael addition to form an open-chain intermediate (C), which undergoes subsequent cyclodehydration losing water giving rise to the formation of desired product (D) (Supplementary information S7).

Table 7 Cellulose[2-(sulfooxy)ethyl]mercaptosulfonic acid[SEMSA] catalyzed one-pot synthesis of hexahydroacridine-1,8-diones

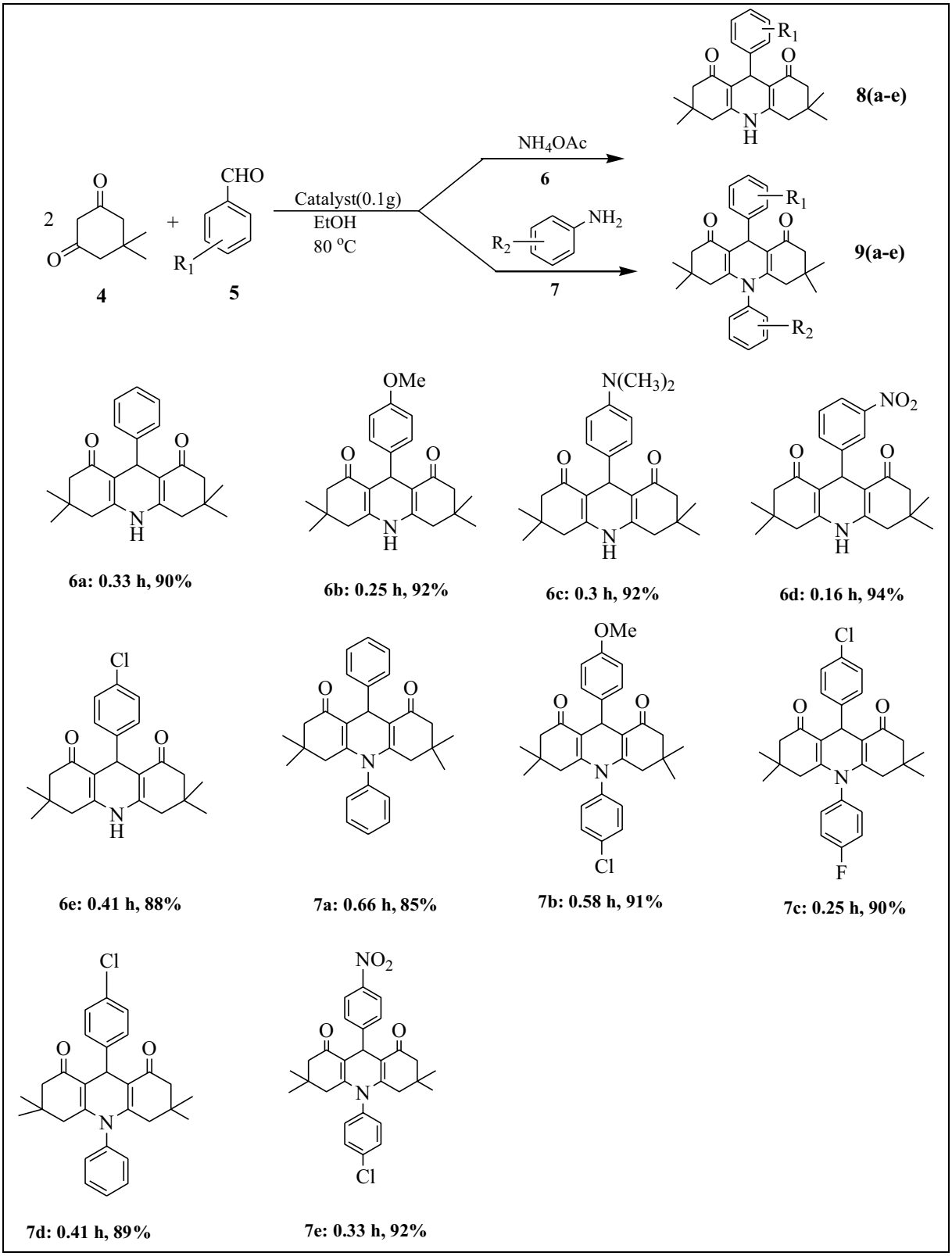

Table 8 Cellulose[2-(sulfooxy)ethyl]mercaptosulfonic acid[SEMSA] catalyzed one-pot synthesis of 1,8-dioxo-octahydroxanthene

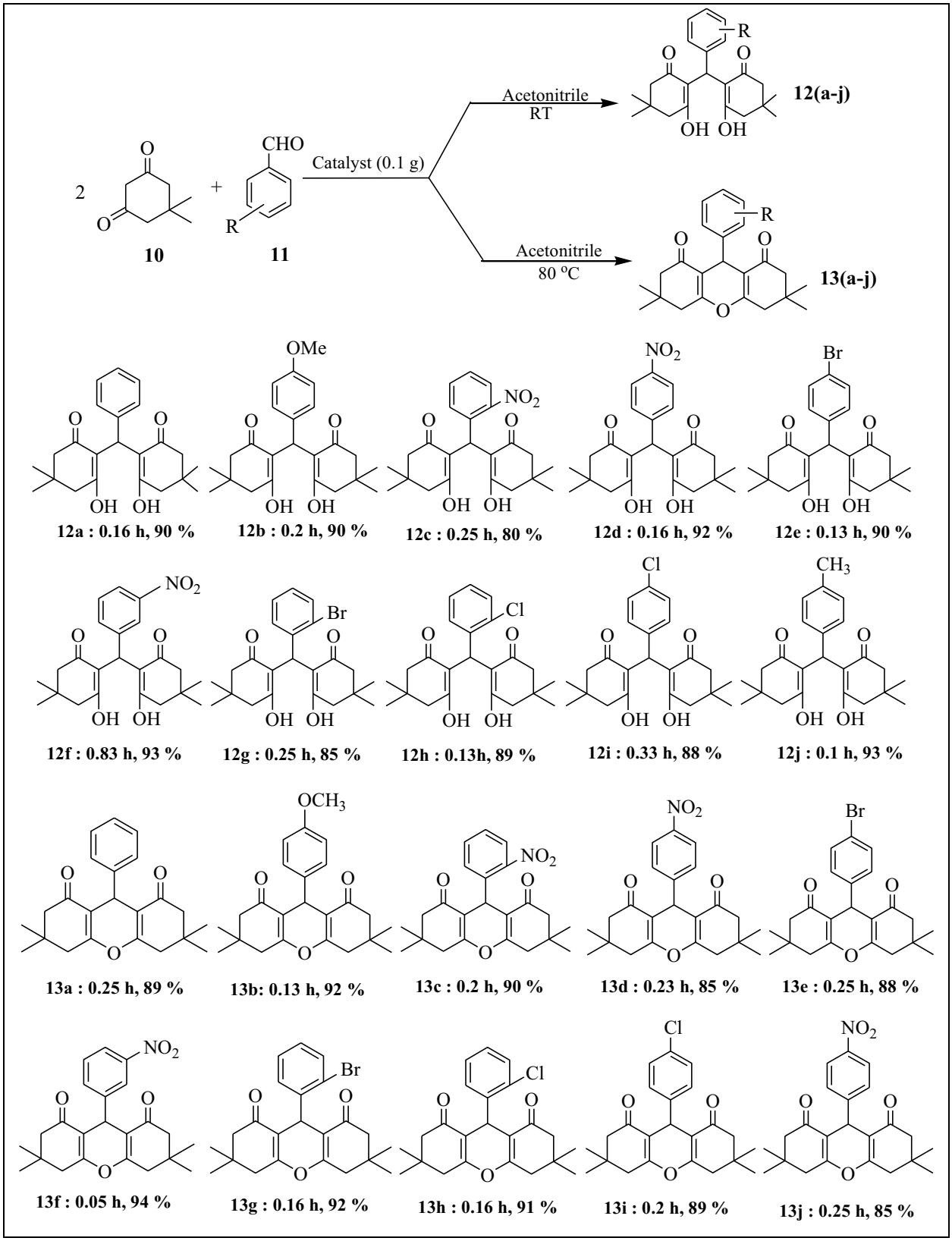

Table 9 Crystallographic data of 2,2′-(4-methoxyphenylmethylene)bis(3-hydroxy-5,5′-dimethyl cyclohexane-1,3-dione)

Bond precision	C–C = 0.0047 A	Wavelength = 0.71073	
Cell	a = 8.9316(13)	b = 11.5871(15)	c = 21.041(3)
	α = 90	β = 98.246(15)	γ = 90
Temperature	293 K		
	Calculated	Reported	
Volume	2155.1(5)	2155.1(5)	
Space group	P 21/n	P 21/n	
Hall group	−P 2yn	−P 2yn	
Moiety formula	C24 H30 O5	C24 H30 O5	
Sum formula	C24 H30 O5	C24 H30 O5	
Mr	398.48	398.48	
Dx, g cm^{-3}	1.228	1.228	
Z	4	4	
Mu (mm^{-1})	0.085	0.085	
F000	856.0	856.0	
F000′	856.43		
h, k, l_{max}	11, 14, 25	11, 14, 25	
N_{ref}	4224	4203	
T_{min}, T_{max}	0.990, 0.992	0.860, 1.000	
T'_{min}	0.983		
Correction method = # Reported T Limits: T_{min} = 0.860 T_{max} = 1.000 AbsCorr = MULTI-SCAN			
Data completeness = 0.995	Theta (max) = 26.000		
R (reflections) = 0.0684(2094)	wR2 (reflections) = 0.2028(4203)		
S = 0.997	Npar = 268		

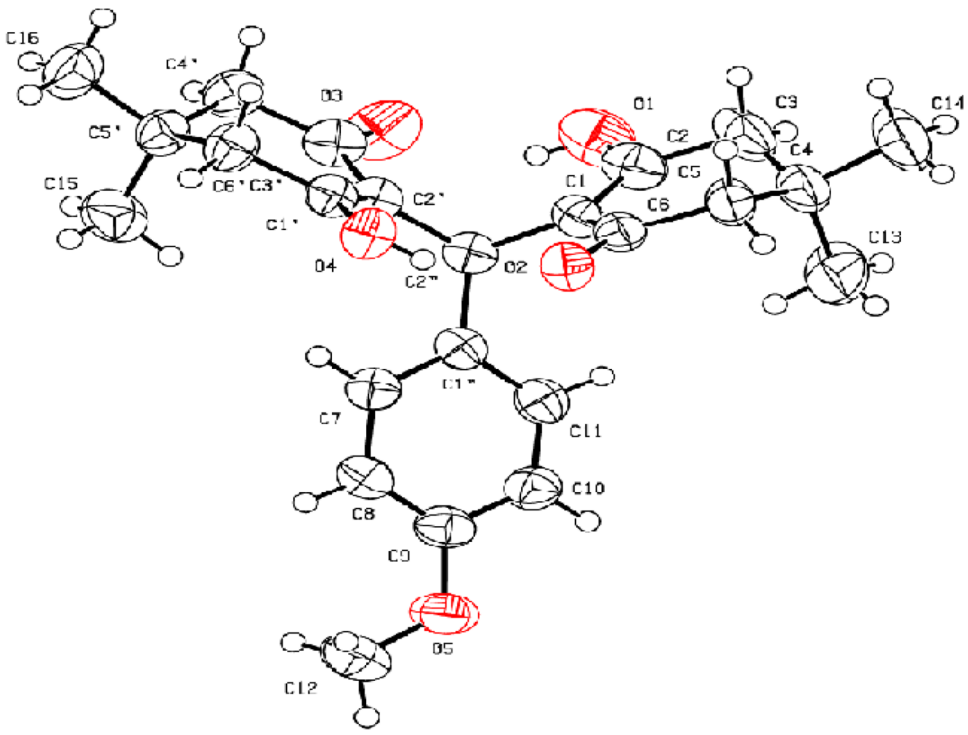

Fig. 10 *ORTEP* view of the molecule with displacement ellipsoids drawn at 50%. H atoms are shown as small spheres of arbitrary radii

Table 10 Crystal and experimental data

CCDC No	1015262
Crystal description	
Crystal size	0.30 x 0.20 x 0.20 mm
Empirical formula	$C_{23}H_{27}ClO_4$
Formula weight	402.90
Radiation, wavelength	MoKα, 0.71073 Å
Unit-cell dimensions	$a = 15.019(5)$, $b = 11.790(5)$, $c = 13.277(5)$ Å
	$\beta = 114.857(5)^o$
Crystal system	Monoclinic
Space group	$P2_1/c$
Unit-cell volume	2133.2(14) $Å^3$
Density (calculated)	1.254 Mgm^{-3}
No. of molecules per unit cell, Z	4
Temperature	293(2) K
Absorption coefficient	0.204 mm^{-1}
$F(000)$	856
Scan mode	ω
θ range for entire data collection	$-3.45° < \theta < 25.0°$
Range of indices	$h = -17$ to 17, $k = -14$ to 8, $l = -11$ to 15
Reflections collected/unique	7748/3733
Reflections observed ($I > 2\sigma(I)$)	1722
R_{int}	0.0625
R_{sigma}	0.1236
Structure determination	Direct methods
Refinement	Full-matrix least-squares on F^2
No. of parameters refined	257
Final R	0.0751
$wR(F^2)$	0.2035
Weight	$1/[\Delta^2(F_o^2) + (0.0672P)^2 + 0.00005P]$
	Where $P = [F_o^2 + 2F_c^2]/3$
Goodness-of-fit	1.010
$(\Delta)_{max}$	0.000
Final residual electron density	$-0.342 < \Delta < 0.352$ $eÅ^{-3}$
Measurement	X'calibur system—Oxford diffraction make, UK
Software for structure solution	SHELXS97 (Sheldrick, 2008)
Software for refinement	SHELXL97 (Sheldrick, 2008)
Software for molecular plotting	ORTEP-3 (Farrugia, 1997)
	PLATON (Spek, 2003)
Software for geometrical calculations	PLATON (Spek, 2003)
	PARST (Nardelli, 1995)

Catalyst testing for the synthesis of 1,8-dioxo-octahydroxanthenes

1,8-Dioxo-octahydroxanthenes were synthesized by stirring a mixture of aldehyde (1 mmol), dimedone (2 mmol) and cellulose[2-(sulfooxy)ethyl]mercaptosulfonic acid[SEMSA] (0.1 g) in a round-bottom flask (100 mL), water (2 mL) was added and the reaction mixture was stirred at room temperature in an oil bath. To select the appropriate catalyst, the reaction with benzaldehyde was selected as the model reaction. Again cellulose[2-(sulfooxy)ethyl]mercaptosulfonic acid[SEMSA] was found to be the best catalyst for the one-pot two-component synthesis of xanthene derivatives both in terms of reaction time and yield (Table 1, entry 5). In order to optimize the amount of cellulose[2-(sulfooxy)ethyl] mercaptosulfonic acid[SEMSA], we carried out the model reaction with varying amounts of catalysts and 0.1 g of cellulose[2-(sulfooxy)ethyl]mercaptosulfonic acid[SEMSA] was found to be the appropriate amount in order to obtain the best results. Further, several organic solvents as reaction

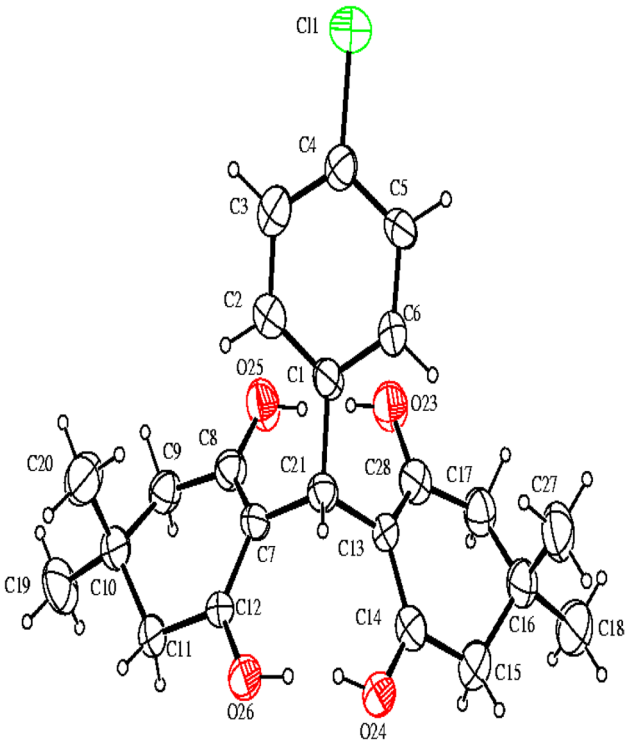

Fig. 11 *ORTEP* view of the molecule with displacement ellipsoids drawn at 40%. H atoms are shown as small spheres of arbitrary radii

media were investigated and found that reaction with acetonitrile gave the best results. To optimize the reaction temperature, this reaction was carried out at RT, 60, 80 and 100 °C and found that at room temperature, an open product was formed and at 80 °C was the optimum reaction temperature for the synthesis of close product (Table 2, entry 2). In order to explore the scope of the designed protocol, a number of commercially available aromatic aldehydes were chosen for the one-pot synthesis of 1,8-dioxo-octahydroxanthenes and the results are summarized in Table 8.

The proposed mechanism for the synthesis of cyclohexen-1-one and 1,8-dioxo-octahydroxanthene involves the formation of hydrogen bonding between the catalyst and the carbonyl oxygen of dimedone during the reaction. Reaction between dimedone and aldehyde leads to the formation of uncyclized intermediate (A) and an open product is formed (B). From this uncyclized intermediate by losing proton leads to the formation of cyclized intermediate and by losing a molecule of water gives rise to the formation of the final close product (C) shown in Scheme 4 of ESM.

Role of nanocatalysts in environmental remediation

Now-a-days, our society faces one of the major problems of environmental pollution. Soil, water and air are totally contaminated by different types of contaminants such as

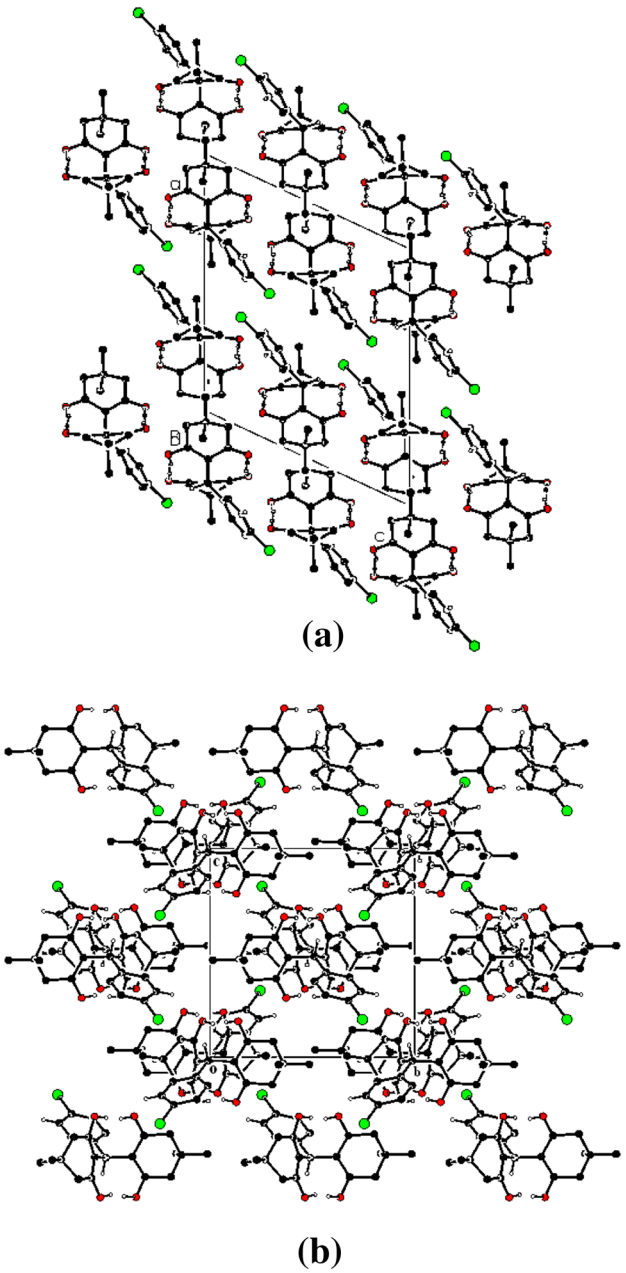

Fig. 12 The packing arrangement of molecules viewed down the **a** b-axis and **b** a-axis

pesticides and fertilizers used in agriculture, metals and toxic gases released in the environment as industrial waste. In order to cope up this situation, new nanotechnologies using nanomaterials have been explored because of their property of large area-to-volume ratio which leads to higher reactivity. Physical and chemical modifications on the surface of nanomaterials have been employed for remediation of pollutants from environment. The present nanotechnology helps in waste water treatment. Nanocatalysts containing metal oxides are used for the sensing and removal of

Table 11 Bond lengths (Å) and bond angles (°) for non-hydrogen atoms (e.s.d.'s are given in parentheses)

Bond lengths	Bond angles	
C(1)–C(2) 1.387(7)	C(2)–C(1)–C(21) 122.3(4)	C(15)–C(16)–C(17) 106.7(4)
C(1)–C(6) 1.374(6)	C(1)–C(2)–C(3) 121.9(5)	C(15)–C(16)–C(18) 109.2(4)
C(1)–C(21) 1.535(6)	C(2)–C(3)–C(4) 118.8(5)	C(15)–C(16)–C(27) 110.3(4)
C(2)–C(3) 1.379(7)	C(3)–C(4)–C(5) 121.0(5)	C(17)–C(16)–C(18) 109.9(5)
C(3)–C(4) 1.374(7)	C(3)–C(4)–CL(1) 120.1(4)	C(17)–C(16)–C(27) 111.3(4)
C(4)–C(5) 1.362(7)	C(5)–C(4)–CL(1) 118.9(4)	C(16)–C(17)–C(28) 115.2(4)
C(4)–CL(1) 1.744(5)	C(4)–C(5)–C(6) 118.7(5)	C(1)–C(21)–C(7) 114.7(4)
C(5)–C(6) 1.376(7)	C(1)–C(6)–C(5) 122.8(5)	C(1)–C(21)–C(13) 113.7(4)
C(7)–C(8) 1.401(6)	C(8)–C(7)–C(12) 118.3(4)	C(7)–C(21)–C(13) 114.4(4)
C(7)–C(12) 1.398(6)	C(8)–C(7)–C(21) 122.1(4)	C(13)–C(28)–C(17) 122.2(5)
C(7)–C(21) 1.523(6)	C(12)–C(7)–C(21) 119.4(4)	C(13)–C(28)–O(23_) 123.9(5)
C(8)–C(9) 1.501(7)	C(7)–C(8)–C(9) 121.9(4)	C(17)–C(28)–O(23_) 113.9(4)
C(8)–O(25_) 1.275(6)	C(7)–C(8)–O(25_) 123.4(4)	
C(9)–C(10) 1.539(7)	C(9)–C(8)–O(25_) 114.8(4)	
C(10)–C(11) 1.523(7)	C(9)–C(10)–C(11) 108.5(4)	
C(10)–C(19) 1.531(7)	C(9)–C(10)–C(19) 108.4(4)	
C(10)–C(20) 1.536(7)	C(9)–C(10)–C(20) 110.6(4)	
C(11)–C(12) 1.491(6)	C(11)–C(10)–C(19) 109.8(4)	
C(12)–O(26_) 1.293(5)	C(19)–C(10)–C(20) 109.0(5)	
C(13)–C(14) 1.393(7)	C(10)–C(11)–C(12) 114.3(4)	
C(13)–C(21) 1.532(6)	C(7)–C(12)–C(11) 122.3(4)	
C(13)–C(28) 1.383(7)	C(7)–C(12)–O(26_) 123.1(4)	
C(14)–C(15) 1.487(7)	C(11)–C(12)–O(26_) 114.6(4)	
C(14)–O(24_) 1.296(6)	C(14)–C(13)–C(21) 119.0(4)	
C(15)–C(16) 1.529(7)	C(14)–C(13)–C(28) 117.3(4)	
C(16)–C(17) 1.526(7)	C(21)–C(13)–C(28) 123.7(4)	
C(16)–C(18) 1.532(7)	C(13)–C(14)–C(15) 122.4(5)	
C(16)–C(27) 1.527(7)	C(13)–C(14)–O(24_) 122.5(5)	
C(17)–C(28) 1.499(7)	C(15)–C(14)–O(24_) 115.1(4)	
C(28)–O(23_) 1.292(6)	C(14)–C(15)–C(16) 114.1(4)	

chemical pollutants by the process of photo-catalysis. The process of removal of pollutants lies behind the fact that morphology of nanomaterials is of different shapes and sizes and they behave as adsorbents. On the other hand when these nanomaterials form catalysts with polymers, these are then used for the removal of gases, biological substances, organic pollutants and harmful chemicals. [117–119].

Crystal structure determination and refinement

In order to grow crystal, we have attempted several times to grow crystals of all compounds from **12a–13j**, but the crystal formed is of the intermediate of one of the compounds **12b**, i.e. 2,2′-(4-methoxyphenylmethylene)bis(3-hydroxy-5,5′-dimethyl-2-cyclohexen-1-one) and the name of the intermediate is 2,2′-(4-methoxyphenylmethylene) bis(3-hydroxy-5,5′-dimethyl cyclohexane-1,3-dione) which is suitable for single-crystal X-ray analysis. The crystal was obtained by crystallization in ethanol solution at room temperature. The structure of the intermediate was determined by single-crystal X-ray diffraction analysis. X-ray intensity data of this compound were collected on a CCD area-detector diffractometer (X'calibur system—Oxford diffraction make, UK) equipped with graphite-monochromated MoKα radiation ($\lambda = 0.71073$ Å) at room temperature.

The compound, C_{24} H_{30} O_5, crystallizes in the monoclinic space group P $2_1/n$ with the following unit-cell parameters: $a = 8.9316(13)$, $b = 11.5871(15)$, $c = 21.041(3)$ Å, $\beta = 98.246(15)^o$ and $Z = 4$. The crystal structure was solved by direct methods using single-crystal X-ray diffraction data collected at room temperature and refined by full-matrix least-squares procedures to a final R-value of 0.0684 for 2094 observed reflections.

X-ray intensity data of 8604 reflections (of which 4203 unique) were collected on *X'calibur* CCD area-detector diffractometer equipped with graphite-monochromated MoKα radiation ($\lambda = 0.71073$ Å). The crystal used for data collection was of dimensions 0.20 X 0.10 X 0.10 mm. 2094

Table 12 Torsion angles (°) for non-hydrogen atoms (e.s.d.'s are given in parentheses)

C(6)–C(1)–C(2)–C(3) 3.6
C(12)–C(7)–C(21)–C(1) − 132.4
C(2)–C(1)–C(6)–C(5) − 4.5
C(21)–C(1)–C(2)–C(3) 178.4
C(2)–C(1)–C(21)–C(7) 20.8
C(2)–C(1)–C(21)–C(13) 155.0
C(21)–C(1)–C(6)–C(5) − 179.4
C(6)–C(1)–C(21)–C(7) − 164.6
C(6)–C(1)–C(21)–C(13) − 30.4
C(1)–C(2)–C(3)–C(4) 0.0
C(2)–C(3)–C(4)–C(5) − 3.0
C(2)–C(3)–C(4)–CL(1) 176.1
C(3)–C(4)–C(5)–C(6) 2.3
CL(1)–C(4)–C(5)–C(6) − 176.9
C(4)–C(5)–C(6)–C(1) 1.6
C(12)–C(7)–C(8)–C(9) 10.8
C(8)–C(7)–C(12)–C(11) − 10.0
C(12)–C(7)–C(8)–O(25_) − 167.5
C(8)–C(7)–C(12)–O(26_) 167.6
C(8)–C(7)–C(21)–C(1) 52.2
C(21)–C(7)–C(8)–C(9) − 173.8
C(8)–C(7)–C(21)–C(13) − 81.6
C(21)–C(7)–C(8)–O(25_) 7.9
C(21)–C(7)–C(12)–C(11) 174.5
C(12)–C(7)–C(21)–C(13) 93.7
C(21)–C(7)–C(12)–O(26_) − 7.9
C(7)–C(8)–C(9)–C(10) 19.2
O(25_)–C(8)–C(9)–C(10) − 162.4
C(8)–C(9)–C(10)–C(11) − 46.9
C(8)–C(9)–C(10)–C(19) − 166.2
C(8)–C(9)–C(10)–C(20) 74.4
C(9)–C(10)–C(11)–C(12) 47.8
C(19)–C(10)–C(11)–C(12) 166.2
C(20)–C(10)–C(11)–C(12) − 73.6
C(10)–C(11)–C(12)–C(7) − 21.1
C(10)–C(11)–C(12)–O(26_) 161.1
C(14)–C(13)–C(21)–C(1) 137.7
C(14)–C(13)–C(21)–C(7) − 88.0
C(21)–C(13)–C(14)–C(15) − 172.5
C(21)–C(13)–C(14)–O(24_) 9.3
C(28)–C(13)–C(14)–C(15) 10.5
C(14)–C(13)–C(28)–C(17) − 14.6
C(14)–C(13)–C(28)–O(23_) 166.2
C(28)–C(13)–C(14)–O(24_) − 167.7
C(28)–C(13)–C(21)–C(1) − 45.6
C(28)–C(13)–C(21)–C(7) 88.8
C(21)–C(13)–C(28)–C(17) 168.6
C(21)–C(13)–C(28)–O(23_) − 10.6
C(13)–C(14)–C(15)–C(16) 23.7
O(24_)–C(14)–C(15)–C(16) − 157.9
C(14)–C(15)–C(16)–C(17) − 49.7
C(14)–C(15)–C(16)–C(18) − 168.6
C(14)–C(15)–C(16)–C(27) 71.4
C(15)–C(16)–C(17)–C(28) 46.2
C(18)–C(16)–C(17)–C(28) 164.6
C(16)–C(17)–C(28)–O(23_) 163.4

reflections were treated as observed ($I > 2\sigma(I)$). Data were corrected for Lorentz, polarization and absorption factors. The structure was solved by direct methods using SHELXS97 [1]. All non-hydrogen atoms of the molecule were located in the best E-map. Full-matrix least-squares refinement was carried out using SHELXL97 [1]. The final refinement cycles converged to an $R = 0.0684$ and $wR(F^2) = 0.2028$ for the observed data. Residual electron densities ranged from $0.181 < \delta\rho < 0.212$ eÅ^{-3}. Atomic scattering factors were taken from International Tables for X-ray Crystallography (1992, Vol. C, Tables 4.2.6.8 and 6.1.1.4). The crystallographic data are summarized in Table 9.

An ORTEP view of the compound with atomic labeling is shown in Fig. 6. The geometry of the molecule was calculated using the WinGX [3], PARST [4] and PLATON [5] software (Fig. 10).

Crystal structure of 2,2′-(4′-chlorophenylmethylene) bis(3-hydroxy-5,5′-dimethyl-2-cyclohexen-1-one) (12i)

X-ray intensity data of 7748 reflections (of which 3733 unique) were collected at room temperature on a CCD area-detector diffractometer (X'calibur system—Oxford diffraction make, U.K.) equipped with graphite-monochromated MoKα radiation ($\lambda = 0.71073$ Å). The crystal used for data collection was of dimensions $0.30 \times 0.20 \times 0.20$ mm. The intensities were measured by Δ scan mode for Δ ranges 3.45°–25.0°. 1722 reflections were treated as observed ($I > 2\sigma$ (I)). Data were corrected for Lorentz and polarization factors. The structure was solved by direct methods using SHELXS97. All non-hydrogen atoms of the molecule were located in the best E-map. Full-matrix least-squares refinement was carried out using SHELXL97. All the hydrogen atoms were geometrically fixed and allowed to ride on the corresponding non-hydrogen atoms with C–H = 0.93–0.98 Å, and $U_{iso} = 1.5U_{eq}$ of the attached C atom for methyl H atoms and 1.2 U_{eq} for other H atoms. The final refinement cycles converged to an $R = 0.0751$ and $wR\ (F^2) = 0.2035$ for the observed data. Residual electron densities ranged from − 0.342 to 0.352 eÅ^{-3}. Atomic scattering factors were taken from International Tables for X-ray Crystallography (1992, Vol. C, Tables 4.2.6.8 and 6.1.1.4).

Table 13 Bond lengths (Å) and bond angles (°) for hydrogen atoms (e.s.d.'s are given in parentheses)

Bond lengths	Bond angles	
C(2)–H(2) 0.930(5)	C(1)–C(2)–H(2) 119.0(5)	C(16)–C(18)–H(18B) 109.5(5)
C(3)–H(3) 0.930(5)	H(2)–C(2)–C(3) 119.0(5)	C(16)–C(18)–H(18C) 109.5(5)
C(5)–H(5) 0.930(5)	C(2)–C(3)–H(3) 120.6(5)	H(18A)–C(18)–H(18B) 109.5(6)
C(6)–H(6) 0.930(5)	H(3)–C(3)–C(4) 120.6(5)	H(18A)–C(18)–H(18C) 109.5(6)
C(9)–H(9A) 0.970(5)	C(4)–C(5)–H(5) 120.7(5)	H(18B)–C(18)–H(18C) 109.5(6)
C(9)–H(9B) 0.970(5)	H(5)–C(5)–C(6) 120.6(5)	C(10)–C(19)–H(19A) 109.5(5)
C(11)–H(11A) 0.970(5)	C(1)–C(6)–H(6) 118.6(5)	C(10)–C(19)–H(19B) 109.5(5)
C(11)–H(11B) 0.970(5)	C(5)–C(6)–H(6) 118.6(5)	C(10)–C(19)–H(19C) 109.5(5)
C(15)–H(15A) 0.970(5)	C(8)–C(9)–H(9A) 108.7(4)	H(19A)–C(19)–H(19B) 109.5(6)
C(15)–H(15B) 0.970(5)	C(8)–C(9)–H(9B) 108.7(4)	H(19A)–C(19)–H(19C) 109.5(5)
C(17)–H(17A) 0.970(5)	H(9A)–C(9)–H(9B) 107.6(5)	H(19B)–C(19)–H(19C) 109.5(6)
C(17)–H(17B) 0.970(5)	H(9A)–C(9)–C(10) 108.7(4)	C(10)–C(20)–H(20A) 109.5(5)
C(18)–H(18A) 0.960(6)	H(9B)–C(9)–C(10) 108.7(4)	C(10)–C(20)–H(20B) 109.5(5)
C(18)–H(18B) 0.960(6)	C(10)–C(11)–H(11A) 108.7(4)	C(10)–C(20)–H(20C) 109.5(5)
C(18)–H(18C) 0.960(6)	C(10)–C(11)–H(11B) 108.7(4)	H(20A)–C(20)–H(20B) 109.5(5)
C(19)–H(19A) 0.960(6)	H(11A)–C(11)–H(11B) 107.6(5)	H(20A)–C(20)–H(20C) 109.5(5)
C(19)–H(19B) 0.960(6)	H(11A)–C(11)–C(12) 108.7(4)	H(20B)–C(20)–H(20C) 109.5(5)
C(19)–H(19C) 0.960(6)	H(11B)–C(11)–C(12) 108.7(4)	C(1)–C(21)–H(21) 104.1(4)
C(20)–H(20A) 0.960(5)	C(14)–C(15)–H(15A) 108.7(5)	C(7)–C(21)–H(21) 104.1(4)
C(20)–H(20B) 0.960(6)	C(14)–C(15)–H(15B) 108.7(5)	C(13)–C(21)–H(21) 104.1(4)
C(20)–H(20C) 0.960(6)	H(15A)–C(15)–H(15B) 107.6(5)	C(16)–C(27)–H(27A) 109.5(5)
C(21)–H(21) 0.980(5)	H(15A)–C(15)–C(16) 108.7(5)	C(16)–C(27)–H(27B) 109.5(5)
C(27)–H(27A) 0.960(6)	H(15B)–C(15)–C(16) 108.7(5)	C(16)–C(27)–H(27C) 109.5(5)
C(27)–H(27B) 0.960(5)	C(16)–C(17)–H(17A) 108.5(5)	H(27A)–C(27)–H(27B) 109.5(5)
C(27)–H(27C) 0.960(5)	C(16)–C(17)–H(17B) 108.5(5)	H(27A)–C(27)–H(27C) 109.5(5)
O(23_)–H(23_) 0.820(4)	H(17A)–C(17)–H(17B) 107.5(5)	H(27B)–C(27)–H(27C) 109.5(5)
O(24_)–H(24_) 0.820(3)	H(17A)–C(17)–C(28) 108.5(5)	C(28)–O(23_)–H(23_) 109.5(4)
O(25_)–H(25_) 0.820(4)	H(17B)–C(17)–C(28) 108.5(5)	C(14)–O(24_)–H(24_) 109.5(4)
O(26_)–H(26_) 0.820(4)	C(16)–C(18)–H(18A) 109.5(5)	C(8)–O(25_)–H(25_) 109.5(4)
		C(12)–O(26_)–H(26_) 109.5(4)

Table 14 C–H…O hydrogen bonding geometry (e.s.d's in parenthesis)

D-H…A	D-H (Å)	D…A (Å)	H…A (Å)	D-H…A (°)
C21–H21…O24	0.98(4)	2.850(6)	2.438(4)	104.8(3)
C21–H21…O26	0.98(4)	2.867(5)	2.412(3)	107.8(2)
O23–H23…O25	0.82(3)	2.608(5)	1.799(3)	168.7(3)
O24–H24…O26	0.82(3)	2.579(5)	1.785(3) 162.7(2)	
O25–H25…O23	0.82(3)	2.608(5)	1.814(3)	162.6(3)
O26–H26…O24	0.82(3)	2.579(5)	1.767(3)	170.9(2)
C5–H5…O24[i]	0.93 (4)	3.250(5)	2.413(3)	149.7(3)

Symmetry code: (i) $x, -y+3/2, z-1/2$

The crystallographic data are summarized in Table 10. CCDC—1015262 contains the supplementary crystallographic data for this paper.

An ORTEP view of the title compound with atomic labeling is shown in Fig. 11. The geometry of the molecule was calculated using the WinGX and PARST software's (Fig. 12, Tables 11, 12, 13, 14).

All the four oxygen atoms are equivalent and have only partial double-bond character. The 2H-atoms are equally shared between all the four oxygen atoms with each H-atom getting 0.5 as occupancy.

Recyclability of the catalyst

In order to study catalyst as pure heterogeneous nanocatalyst, recyclability of the catalyst required to be examined. After completion of the reaction, the catalyst could be easily separated by simple filtration, washed with distilled water, dried and could be reused for subsequent runs. A series

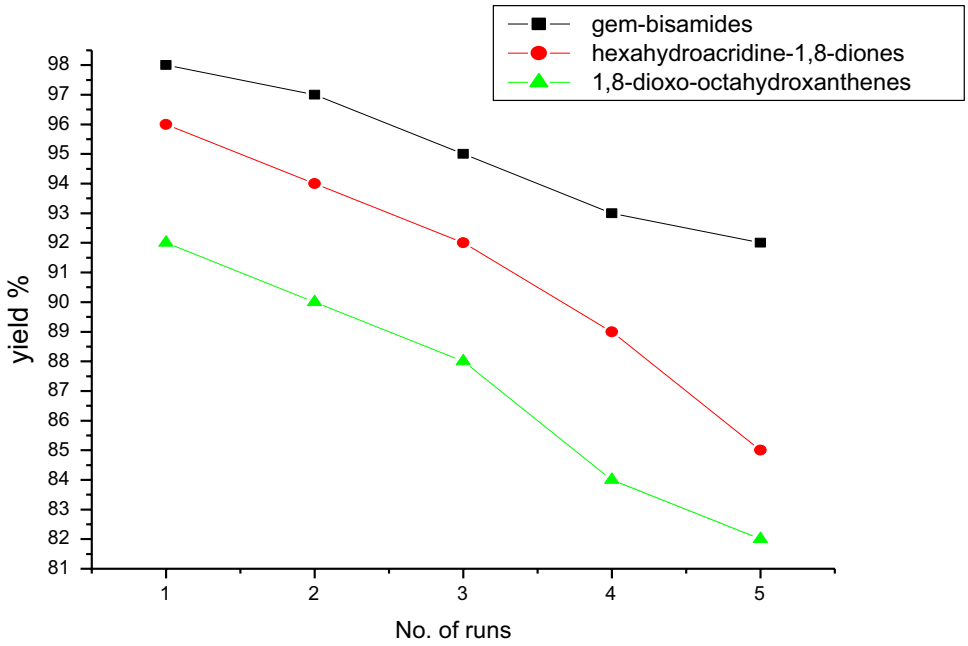

Fig. 13 Recyclability of carbon-based nanocatalyst, i.e. cellulose[2-(sulfooxy)ethyl]mercaptosulfonic acid[SEMSA] for the synthesis of *gem*-bisamides, hexahydroacridine-1,8-diones and 1,8-dioxo-octahydroxanthenes

of five consecutive runs were carried out in case of *gem*-bisamides using benzaldehyde (1 mmol) and benzamide (2 mmol) as test substrates, hexahydroacridine-1,8-diones using dimedone (2 mmol), aromatic aldehyde (1 mmol), ammonium acetate (1 mmol) as test substrate and 1,8-dioxo-octahydroxanthenes using aldehyde (1 mmol) and dimedone (2 mmol) as test substrate. It was found that a little drop in the activity of the catalyst observed after every run. The results are shown in Fig. 7.

The prepared nanocatalyst is recyclable up to five consecutive runs, and recyclability was confirmed by HR-TEM. Moreover, the catalyst is active for almost all the aromatic aldehydes (Fig. 13).

Conclusion

We conclude the work by developing an efficient carbon-based nanocatalyst, i.e. cellulose[2(sulfooxy)ethyl]mercaptosulfonic acid[SEMSA] from starting materials, which have easy availability with a simple methodology and thorough characterization using many studies. Nanocatalysts are explored at an alarming rate for their property of high surface area and high reactivity. The application of this nanocatalyst was applied to evaluate many organic transformations such as synthesis of *gem*-bisamides, hexahydroacridine-1,8-diones under milder conditions and excellent yield of products were obtained. Moreover, synthesis of 1,8-dioxo-octahydroxanthenes has been successfully obtained too and crystal of an intermediate also obtained. The prepared nanocatalyst also showed good activity and could be recovered and recycled up to fifth run with little drop in activity after every run which made the process cost-effective. HR-TEM also confirmed the recyclability of the catalyst and found that there occurs the aggregation of the catalyst leads to the formation of rod-shaped structures with slight change in activity of this catalyst.

Acknowledgements I am grateful to Director, SAIF, IIT Bombay for SEM, TEM. I also extend my thanks to Prof. R. K. Bamezai, Department of Chemistry, University of Jammu for recording TGA. I am thankful to Prof. H. N. Sheikh for providing me the FTIR analysis. We are also thankful to the department of Physics for providing us the XRD data of the crystal and Dr. Amit Kumar Sharma for providing me the NMR data of the prepared compounds.

References

1. G. Kour, M. Gupta, Dalton Trans. **46**, 7039 (2017)
2. J.H. Clark, Pure Appl. Chem. **73**, 103–111 (2001)
3. J.A. Melero, R. Grieken, G. Morales, Chem. Rev. **106**, 3790–3812 (2006)
4. S. Pathak, K. Debnath, A. Pramanik, Beilstein J. Org. Chem. **9**, 2344–2353 (2013)
5. M. Kour, S. Paul, New J. Chem. **39**, 6338–6350 (2015)
6. J. Cybulski, M. Cybulski, M. Sharma, R.A. Sheldon, *Fine Chemicals Manufacture: Technology and Engineering*, 1st edn. (Elsevier, Amsterdam, 2001)
7. D.M. Pore, U.V. Desai, T.S. Thopate, P.P. Wadgaonka, Synth. Commun. **34**, 2135–2142 (2004)
8. A.D. Sagar, S.N. Chamle, M.V. Yadav, J. Chem. Pharm. Res. **5**, 156–160 (2013)
9. J.H. Clark, Acc. Chem. Res. **35**, 791–797 (2002)
10. M.R. Mohammadizadeh, A. Hasaninejad, M. Bahramzadeh, Z.S. Khanjarlu, Synth. Commun. **39**, 1152–1165 (2009)

11. S.N. Sadat, F. Hatamjafari, Orient. J. Chem. **31**, 1191–1193 (2015)
12. A. Maleki, M. Kamalzare, Tetrahedron Lett. **55**, 6931–6934 (2014)
13. A. Maleki, H. Movahed, P. Ravaghi, T. Kari, RSC Adv. **6**, 98777–98787 (2016)
14. A. Maleki, M. Aghaei, R. Paydar, J. Iran. Chem. Soc. **14**, 485–490 (2017)
15. A. Maleki, P. Ravaghi, M. Aghaei, H. Movahed, Res. Chem. Intermed. **43**, 5485–5494 (2017)
16. A. Maleki, H. Movahed, P. Ravaghi, Carbohydr. Polym. **156**, 259–267 (2017)
17. A. Maleki, A.A. Jafari, S. Yousefi, Carbohydr. Polym. **175**, 409–416 (2017)
18. A. Maleki, P. Ravaghi, H. Movahed, Micro Nano Lett. **13**, 591–594 (2018)
19. A. Maleki, Ultrason. Sonochem. **40**, 460–464 (2017)
20. A. Maleki, V. Eskandarpour, J. Rahimi, N. Hamidi, Carbohydr. Polym. **208**, 251–260 (2018)
21. W.J. Lee, U.N. Maiti, J.M. Lee, J. Lim, T.H. Han, S.O. Kim, Chem. Commun. **50**, 6818–6830 (2014)
22. M. Okamura, A. Takagaki, M. Toda, J.N. Kondo, K. Domen, T. Tatsumi, M. Hara, S. Hayashi, Chem. Mater. **18**, 3039–3045 (2006)
23. M. Toda, A. Takagaki, M. Okamura, J.N. Kondo, S. Hayashi, K. Hayashi, M. Hara, Nature **438**, 178 (2005)
24. A. Takagaki, M. Takagaki, M. Okamura, J.N. Kondo, S. Hayashi, K. Domen, M. Hara, Catal. Today **116**, 157–161 (2006)
25. S. Suganuma, K. Nakajima, M. Kitano, D. Yamaguchi, H. Kato, S. Hayashi, M. Hara, J. Am. Chem. Soc. **130**, 12787–12793 (2008)
26. S. Suganuma, K. Nakajima, M. Kitano, D. Yamaguchi, H. Kato, S. Hayashi, M. Hara, Solid State Sci. **12**, 1029–1034 (2010)
27. D. Yamaguchi, M. Hara, Solid State Sci. **12**, 1018–1023 (2010)
28. K. Nakajima, M. Hara, ACS Catal. **2**, 1296–1304 (2012)
29. P.A. Russo, M.M. Antunes, P. Neves, P.V. Wiper, E. Fazio, F. Neri, F. Barreca, L. Mafra, M. Pillinger, N. Pinna, A.A. Valente, Green Chem. **16**, 4292–4305 (2014)
30. P. Gupta, S. Paul, Green Chem. **13**, 2365–2372 (2011)
31. T. Yamazaki, K.Y. Numani, M. Goodman, Biopolymers **31**, 1513–1528 (1991)
32. C.A.G.N. Montalbeti, V. Falque, Tetrahedron **61**, 10827–10852 (2005)
33. J.R. Satam, R.V. Jayaram, Catal. Commun. **9**, 2365–2370 (2008)
34. F. Tamaddon, F. Aboee, A. Nasiri, Catal. Commun. **16**, 194–197 (2011)
35. J.W. Bode, Curr. Opin. Drug Discov. Devel. **9**, 765–775 (2006)
36. H.R. Shaterian, M. Ghashang, M. Feyzi, Appl. Catal. A **345**, 128–133 (2008)
37. T. Dingermann, D. Steinhilber, G. Folkers, *Molecular Biology in Medicinal Chemistry*, vol. 21 (Wiley-VCH, Weinheim, 2004), pp. 381–398
38. A.Y. Shen, C.L. Chen, C.I. Lin, Chin. J. Physiol. **35**, 45–54 (1992)
39. F. Al-Assar, K.N. Zelenin, E.E. Lesiovskaya, I.P. Bezhan, B.A. Chakchir, Pharm. Chem. J. **36**, 598–603 (2002)
40. P.V. Pallai, R.S. Struthers, M. Goodman, L. Moroder, E. Wunsch, W. Vale, Biochemistry **24**, 1933–1941 (1985)
41. M. Sechi, U. Azzena, M.P. Delussu, R. Dallocchio, A. Dessi, A. Cosseddu, N. Pala, N. Neamati, Molecules **13**, 2442–2461 (2008)
42. C. Aleman, J. Puiggali, J. Org. Chem. **60**, 910–924 (1995)
43. N.P. Selvam, S. Saranya, P.T. Perumal, Can. J. Chem. **85**, 32–38 (2008)
44. H.R. Sadaati-Mosgtaghin, F.M. Zonoz, M.M. Amini, J. Solid State Chem. **260**, 16–22 (2018)
45. B. Maleki, M. Bhagayeri, RSC Adv. **5**, 79746–79758 (2015)
46. H.A. Soliman, A.Y. Mubarak, S.S. Elmorsy, Chin. Chem. Lett. **27**, 353–356 (2016)
47. R.P. Bakhshani, A. Hassanabadi, J. Chem. Res. **40**, 35 (2016)
48. T.L. Lambat, S.S. Deo, F.S. Inam, T.B. Deshmukh, A.R. Bhat, Karbala Int. J. Mod. Sci. **2**, 63–68 (2016)
49. F.M. Moghaddam, G. Tavakoli, B. Saeednia, Chem. Sel. **2**, 1316–1322 (2017)
50. G. Ramachandran, R. Saraswathi, M. Kumarraja, P. Govindaraj, T. Subramanian, Synth. Commun. **48**, 216–222 (2018)
51. B. Mohammadi, B.R. Khorrami, Montash. Chem. **149**, 1089 (2018)
52. J. Ungar, F. Robinson, J. Pharmacol. Exp. Ther. **80**, 217–232 (1944)
53. I. Antonini, P. Polucci, L.R. Kelland, E. Menta, N. Pescalli, S. Martelli, J. Med. Chem. **42**, 2535–2541 (1999)
54. P.J. McCarthy, T.P. Pitts, G.P. Gunawardana, M. Kelly-Borges, S.A. Pomponi, J. Nat. Prod. **55**, 1664–1668 (1992)
55. D.P. Spalding, E.C. Chapin, H.S. Mosher, J. Org. Chem. **19**, 357 (1954)
56. N. Filloux, J.P. Galy, Synlett **9**, 1137–1139 (2001)
57. I. Antonini, P. Polucci, A. Magnano, D. Cacciamani, M.T. Konieczny, J. Paradziej-Łukowicz, S. Martelli, Bioorg. Med. Chem. **11**, 399–405 (2003)
58. M.A. Pasha, R.R. Khan, K.B. Ramesh, Can. Chem. Trans. **4**, 90–98 (2016)
59. S. Rahmani, A. Amoozadeh, J. Nanostruct. **4**, 83–93 (2014)
60. M. Nasr-Esfahani, M. Montazerozohori, T. Abdizadeh, C. R. Chimie **18**, 547–553 (2015)
61. M. Kiani, M. Mohammadipour, RSC Adv. **7**, 997–1007 (2017)
62. R. Sarada, V. Jagannadharao, B. Govindh, M. Padma, Int. J. Chemtech. Res. **10**, 1011–1117 (2017)
63. A. Jain, S. Singh, K.R. Tiwari, N. Kumar, R. Tomar, Int. J. Mater. Sci. **13**, 189–204 (2018)
64. R. Karmakar, A. Bhaumik, B. Banerjee, C. Mukhopadhyay, Tetrahedron Lett. **58**, 622–628 (2017)
65. H. Sharghi, P. Shiri, M. Aberi, Beilstein J. Org. Chem. **14**, 2745–2770 (2018)
66. K. Nikoofar, F.M. Yielzoleh, J. Saudi Chem. Soc. **22**, 715–741 (2018)
67. M. Mokhtary, Acad. J. Polym. Sci. **2**, 555580 (2018)
68. A. Murugesan, R.M. Gengan, K.G. Moodley, G. Gericke, Adv. Mater. Lett. **8**, 773–782 (2017)
69. H. Singh, H. Singh, A. Singh, M.K. Gupta, S. Sharma, P.M.S. Bedi, Indian J. Pharm. Sci. **79**, 801–812 (2017)
70. S. Mao, F. Li, Y. Lv, C. Lv, S. Yu, Heterocycles **94**, 1895–1902 (2017)
71. F. Hatamjafari, O.H. Lazarjani, Rev. Roum. Chim. **62**, 255–260 (2017)
72. G.J. Bennett, H.H. Lee, Phytochemistry **28**, 967–998 (1989)
73. Y. Na, J. Pharm. Pharmacol. **61**, 707–712 (2009)
74. A.N. Dadhania, V.K. Patel, D.K. Raval, J. Saudi Chem. Soc. **21**, S163–S169 (2017)
75. S. Samantaray, P. Kar, G. Hota, B.G. Mishra, Ind. Eng. Chem. Res. **52**, 5862–5870 (2013)
76. O. Sirkecioglu, N. Talinli, A. Akar, J. Chem. Res. **86**, 502–506 (1995)
77. A. Banerjee, A.K. Mukherjee, Stain Technol. **56**, 83–85 (1981)
78. J. Liu, Z. Diwu, W.Y. Leung, Bioorg. Med. Chem. Lett. **11**, 2903–2905 (2001)
79. G. Song, B. Wang, H. Luo, L. Yang, Catal. Commun. **8**, 673–676 (2007)
80. S. Kantevari, R. Bantu, L. Nagarapu, Arkivoc **16**, 136–148 (2006)

81. F. Nemati, S. Sabaqian, J. Saudi Chem. Soc. **21**, S383–S393 (2017)
82. S. Maripi, R.B. Korupolu, S.B. Madasu, GSC **7**, 70–84 (2017)
83. A.B. Waghamare, S.S. Deshmukh, G.M. Bondle, A.V. Chate, Chem. Biol. Interact. **8**, 151–153 (2018)
84. S.V. Deshmukh, G.K. Kadam, S.V. Shisodia, M.V. Katarina, S.B. Vbale, R.P. Pawar, Int. J. Phys. Chem. Sci. **7**, 75 (2018)
85. B.M. Sapkal, A.J. Sahani, A.S. Burange, S. Kale, G. Abraham, S. Disale, Curr. Catal. **7**, 144 (2018)
86. F.N. Sadeh, M. Fatehpour, N. Hazeri, M.T. Maghsoodlou, M. Lashkari, Acta Chem. Iasi **25**, 24 (2017)
87. S. Karhale, M. Patil, G. Rashinkar, V. Helavi, Res. Chem. Intermed. **43**, 7073–7086 (2017)
88. M. Pirouzmand, A.M. Gharehbaba, Z. Ghasemi, S.A. Khaaje, Arab. J. Chem. **10**, 1070 (2017)
89. R.R. Magar, G.T. Pawar, S.P. Gadekar, M.K. Lande, Bull. Chem. React. Eng. Catal. **13**, 436–446 (2018)
90. M.B. Swami, A.H. Jadhav, N.V. Ghule, S.S. Mahurkar, S.R. Mathapati, A.N. Patil, S.G. Patil, IJGHC **7**, 788 (2018)
91. B. Karami, K. Eskandari, G. Ansari, Der. Chemica. Sinica. **8**, 342 (2017)
92. S.B. Pore, Asian J. Chem. **30**, 2621–2624 (2018)
93. S.U. Deshmukh, G.K. Kadam, S.U. Shisodia, M.V. Katarina, S.B. Ubale, R.P. Pawar, IJCPS **7**, 1 (2018)
94. S.M. Vahdat, M. Akbari, Orient. J. Chem. **24**, 1573–1580 (2011)
95. B. Aday, Y. Yildiz, R. Ulus, S. Eris, F. Sen, M. Kaya, New J. Chem. **40**, 748–754 (2016)
96. Y.B. Shen, G.W. Wang, Arkivoc **16**, 1–8 (2008)
97. B. Das, P. Thirupathi, I. Mahender, V.S. Reddy, Y.K. Rao, J. Mol. Catal. A Chem. **247**, 233–239 (2006)
98. S. Kumari, A. Shekhar, D. Pathak, Chem. Sci. Trans. **3**, 652–663 (2014)
99. G.M. Sheldrick, Acta Cryst. A **64**, 112–122 (2008)
100. G. Ramachandran, R. Saraswathi, M. Kumarraja, P. Govindaraj, T. Subramanian, Synth. Commun. **48**, 216–222 (2018)
101. N. Azizi, M. Alipour, J. Mol. Liq. **206**, 268–271 (2015)
102. H.A. Soliman, A.Y. Mubarak, S.S. Elmorsy, Chin. Chem. Lett. **27**, 353–356 (2016)
103. S. Khabnadideh, K. Zomorodian, B.B.F. Mirjalili, E. Izadi, L. Zamani, J. Chil. Chem. Soc. **61**, 3116 (2016)
104. K. Selvakumar, T. Shanmugaprabha, M. Kumaresan, P. Sami, Synth. Commun. **47**, 2115–2126 (2017)
105. A. Khojastehnezhad, F. Moeinpour, M. Vafaei, J. Mex. Chem. Soc. **59**, 29–35 (2015)
106. A.P. Marjani, J. Khalafy, S. Mahmoodi, ARKIVOC **iii**, 262–270 (2016)
107. S.-J. Yü, S. Wu, X.-M. Zhao, C.-W. Lü, Res. Chem. Intermed. **43**, 3121–3130 (2017)
108. G.D. Shirole, S. Bhalekar, S.N. Shelke, Indian J. Chem. **57B**, 1430–1435 (2018)
109. M.A. Mangalavathi, J. Pasha, Chem. Chem. Sci. **8**, 1009–1017 (2018)
110. M. Pirouzmand, A.M. Gharehbaba, Z. Ghasemi, S.A. Khaaje, Arab. J. Chem. **10**, 1070–1076 (2017)
111. F. Nemati, S. Sabaqian, J. Saudi Chem. Soc. **21**, S383–S393 (2017)
112. S. Maripi, R.B. Korupolu, S.B. Madasu, Green Sustain. Chem. **7**, 70–84 (2017)
113. A. Thakur, A. Sharma, A. Sharma, Synth. Commun. **46**, 1766–1771 (2016)
114. R. Khoeiniha, A. Ezabadia, A. Olyaei, Iran. Chem. Commun. **4**, 273–282 (2016)
115. K. Hemalatha, G. Madhumitha, A. Kajbafvala, N. Anupama, R. Sompalle, S.M. Roopan, J. Nanomater. **2013**, 1–23 (2013)
116. S. Erdem, B. Erdem, R.M. Oksuzoglu, Open Chem. **16**, 923–929 (2018)
117. F.D. Guerra, M.F. Attia, D.C. Whitehead, F. Alexis, Molecules **23**, 1760 (2018)
118. P. Singh, M. Abdullah, S. Ikram, Nano Res. Appl. **2**, 1–10 (2016)
119. M.M. Khin, A.S. Nair, V.J. Babu, R. Murugana, S. Ramakrishna, Energy Environ. Sci. **5**, 8075–8109 (2012)